Beach State Report

Quarteira, Praia de Faro and Costa da Caparica

EW-Coast Project

Early warning system for coastal risks induced by storms

ALG-LISBOA-01-145-FEDER- 028657

July 2020

UAlg CIMA
UNIVERSIDADE DO ALGARVE
CENTRO DE INVESTIGAÇÃO MARINHA E AMBIENTAL

LABORATÓRIO NACIONAL
DE ENGENHARIA CIVIL

Beach State Report

Quarteira, Praia de Faro and Costa da Caparica

Juan L. Garzon (UAlg-CIMA)

Andreia M. Marques Ferreira (LNEC)

Óscar Ferreira (UAlg-CIMA)

Conceição Juana Fortes (LNEC)

Maria Teresa Reis (LNEC)

EW-Coast Project

Early warning system for coastal risks induced by storms

ALG-LISBOA-01-145-FEDER- 028657

https://www.cima.ualg.pt/EW-COAST/

July, 2020

TEAM

Coordination

Óscar Ferreira – Main Researcher, UAlg - CIMA

Maria Teresa Reis – Co-Main Researcher, LNEC

UAlg – CIMA

Juan L. Garzon

Susana Costas

A. Rita Carrasco

Luísa Bon de Sousa

Margarida Ramires

LNEC

Conceição Juana Fortes

Andreia M. Marques Ferreira

Liliana V. Pinheiro

Rui Capitão

Rute Lemos

Consultants

Ap van Dongeren – Deltares

Theocharis Plomaritis – University of Cadiz

https://www.cima.ualg.pt/EW-COAST/

List of Contents

List of Figures

List of Tables

1. Introduction and background

Among other factors, the morphology of a sandy beach depends on the current and past wave conditions, the tidal range and the sediment size. Several categories to describe the beach morphology or beach state have been defined in the literature, being the most well know the morphodynamic beach state. In such case, beach states range from dissipative to reflective. Conceptual beach morphodynamic classification models, as the one presented by Masselink and Short (1993), assume that the beach morphodynamics depend on two dimensionless parameters: Ω and RTR (Figure 1). The former is the dimensionless fall velocity and the latter is the relative tide range, which depend on (see Figure 1) Hb and T (breaking significant wave height and peak period), MSR (tidal range) and w_s (sediment fall velocity).

Along the year, the beach morphology evolves to adapt to the incoming wave energy. At beaches with marked seasonality, in winter, when more severe wave conditions occur, the beach profile progresses to a more dissipative state, while in summer, when the wave energy decreases, the beach profile becomes more reflective. However, this change can occur within just a few days/weeks for more reactive beaches. Coarser sediment has larger sediment fall velocity, and therefore, Ω will be reduced. The existence of beach features such as beach cups, berms, sand bars, low terraces, along with the emerged and submerged beach slopes, is also controlled by these two dimensionless parameters.

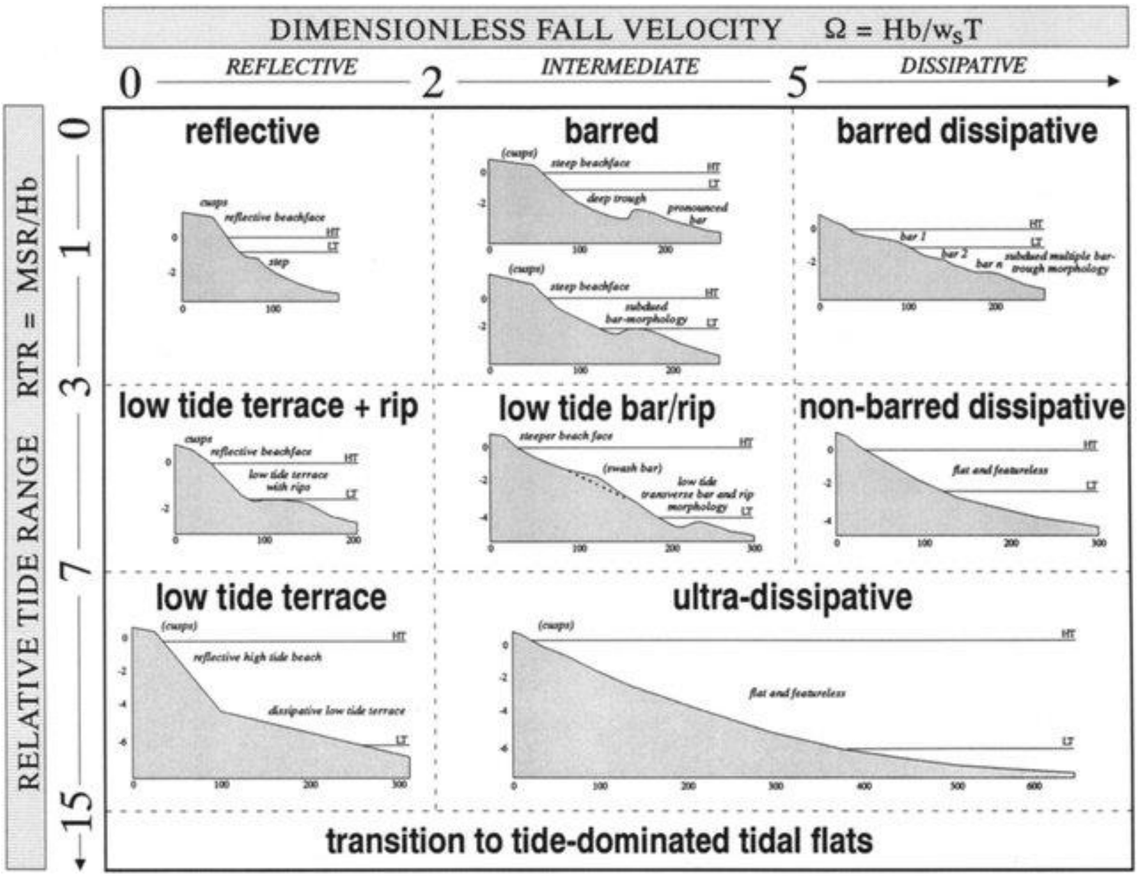

Figure 1. Beach state classification developed by Masselink and Short (1993).

In the long term, each beach presents a dominate state defined by the medium energy conditions in the area, but can also vary between limits depending on existing extremes of wave energy and on sediment availability. Thus, depending on the forcing conditions, the beach morphology will move to more reflective or dissipative states.

This report aims to define beach states for three study areas at the Portuguese coast (Quarteira, Praia de Faro and Costa da Caparica) based on historical information and beach profile measurements carried out at each study site. The beach states will be defined by the dominant morphologies, representing both dominant wave conditions (calm to moderate) and beach morphology after/during high-energy wave conditions. The beach state morphologies defined here will feed the numerical model used to train the Bayesian network under the scope of the EW-Coast project.

2. Case Studies

2.1. Brief description of sites

2.1.1. Quarteira

This site consists of a set of three sandy beaches with a total longshore length of 900 m. The main orientation of the coastline is 118° (north = 0°). The three beaches are laterally limited by 150 m long rock armoured groins. These groins make the three beaches behave almost like “manmade pocket beaches” controlled by groins at their extremities.

During the dominant conditions, the groins maintain the sediment in the system. However, during very energetic conditions, the sediment can fall outside of the system. Beach nourishments have been performed at the area to guarantee a reasonable beach width for bathing conditions.

At the backside, the beach is limited by a long promenade with an elevation ranging from 6 to 8 m above Mean Sea Level (MSL). Beyond this promenade, several touristic facilities are located including restaurants, hotels and supermarkets (Figure 2). While Quarteira is a highly relevant touristic destination in Portugal, the beach morphodynamics have been poorly investigated.

2.1.2. Faro

Praia de Faro is a natural open sandy beach located in the narrow Ancão Peninsula, in the westernmost region of the Ria Formosa. This report focuses on the stretch of the beach where the urban development is more relevant.

The ocean front is partially stabilised with rocks or naturally protected by the dune. The dune elevation varies alongshore with higher elevation at the western portion of the study area, while at the central and eastern parts, the dune is almost destroyed by urban development (Figure 2).

The central part is periodically overwashed during spring tides or storm conditions (Matias *et al.*, 2010; Vousdoukas *et al.*, 2012b). The site presents a steep beach-face, with average slope around 10%, varying from 6% to 15% (Vousdoukas *et al.*, 2012a), with gentler slopes in the eastward side.

In previous studies (Almeida *et al.*, 2012; Vousdoukas et al., 2012a), the western part of the site was classified as reflective during calm conditions and intermediate during energetic conditions, with longshore bar formation. A beach berm can be normally found, except after energetic storms, with a variable width (from less than 15 m to more than 40 m).

The study area has been found to respond rapidly to storm events and variations of the wave forcing. Similarly, the beach can regain in days/weeks a large part of the sediment after the storm events. Moreover, it is characterised by the presence of multiple highly dynamic beach cusps at the lower beach-face that interact with the more persistent, upper beach-face cusps (Vousdoukas *et al.*, 2012a).

Net longshore and littoral drift in the study area are typically eastward, and various estimates have been made of the rate of movement. Results range from 6,000 m^3/year to 380,000 m^3/year, depending on the methodology followed by the authors (Almeida *et al.*, 2012), with an overall average pointing to about 100 000 m^3/year (F. D. Santos et al., 2014). Sediments are medium to very coarse, moderately well sorted sands with median (d50) and mean (D) around 500 µm and d90 around 2,000 µm (Vousdoukas *et al.*, 2012a).

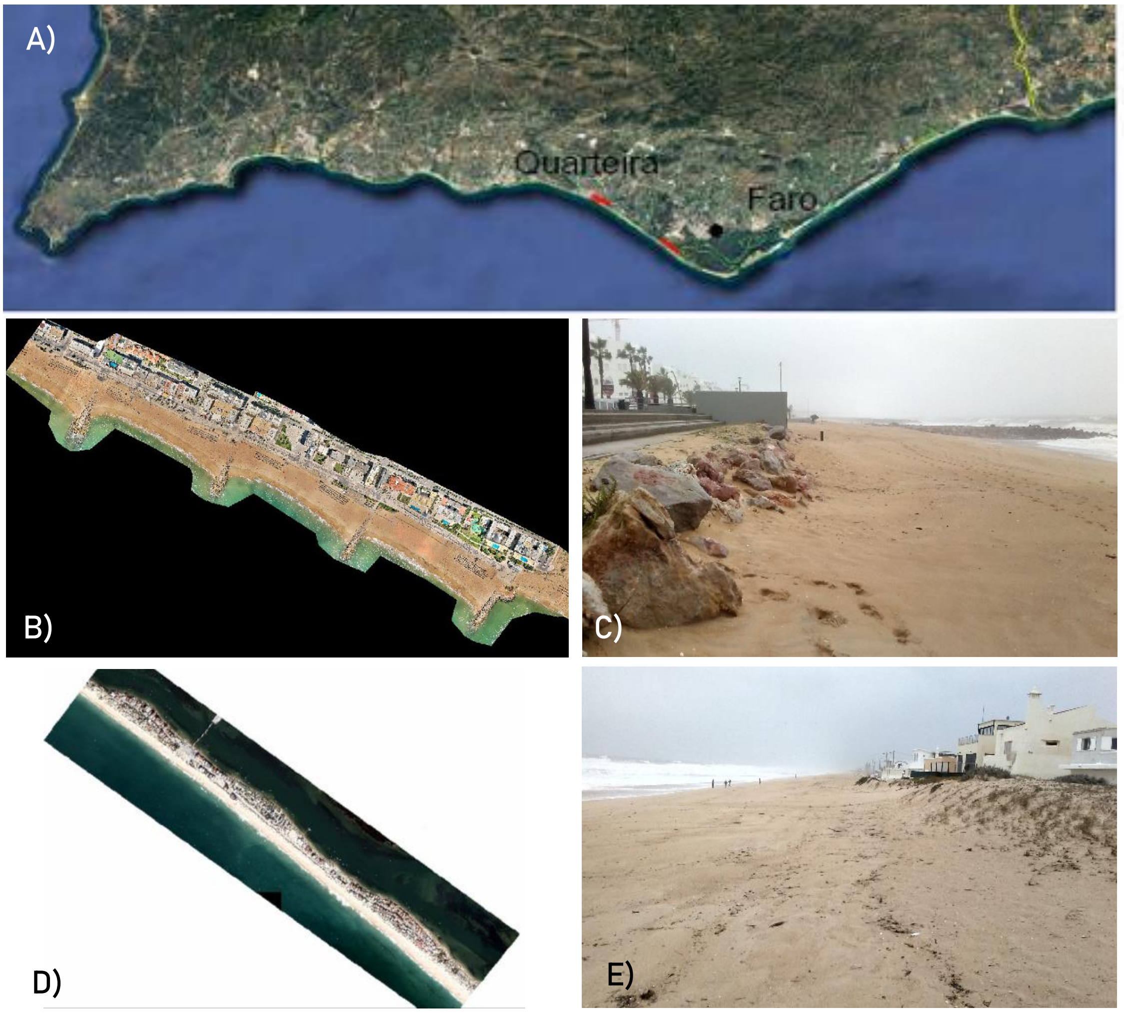

Figure 2. A) Southern Portugal, displaying the location of Faro and Quarteira. B) Three sandy beaches in Quarteira study area. C) Quarteira site with the manmade features and the residential buildings. D) Praia de Faro study area. E) Foredune impacted by human occupation at Praia de Faro.

2.1.3. Costa da Caparica

Costa da Caparica is located on the west coast of mainland Portugal (Figure 3), forming part of a coastal arch with a large radius of curvature, Caparica-Espichel bay, essentially composed by soft detrital rocks (Diogo *et al.*, 2013), and characterised as a low sandy coast. Costa da Caparica nearshore is characterised by very shallow bathymetry.

The study area refers to the urban sector of Costa da Caparica, from the southern section of São João da Caparica beach to the northern section of Nova Praia beach, approximately 2.7 km long, with a predominant NNW-SSE orientation. This entire coastal sector was severely modified with hard defence structures (Figure 4), imposing landward and lateral confinements. The coastline is defended by a longshore rubble mound seawall and a groin field. The groins length varies between 100 m and 250 m. Seawall and groins' crest levels are approximately 6 m and 4 m above MSL, respectively. The groin field creates six sandy cells with a longshore length that varies between 250 m and 400 m.

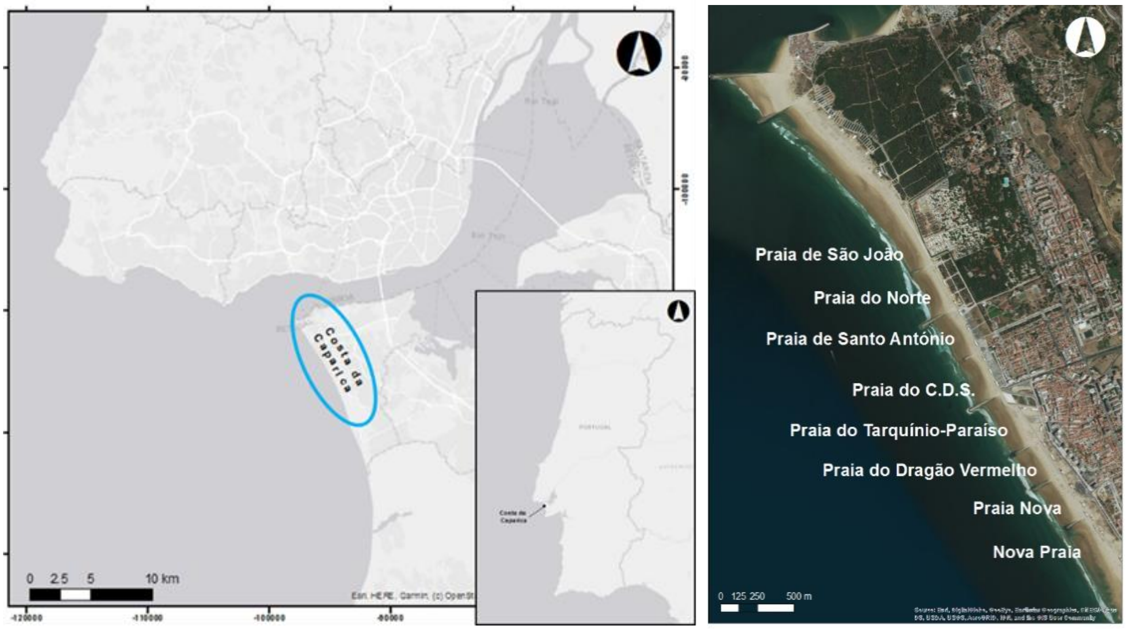

Figure 3. Costa da Caparica study area, with indication of the names of the beaches.

Figure 4. Panoramic aerial view of Costa da Caparica study area. Oblique photography, 07/11/2007 Tires – Arrifana flight (SIARL, 2017).

This urban area is under intensive human pressure, with several beach facilities (e.g. bars and restaurants) located on the seawall crest, accessible all year-round.

Costa da Caparica urban beaches are sensitive to events of extreme oceanographic conditions causing wave overtopping, flooding and beach erosion. Between 2000 and 2019, several events in which wave overtopping and/or erosion occurred have been reported for this site (Ferreira, 2016; Heleno, 2017; Jaranović, 2017; Pinto *et al.*, 2014). In total, 26 documented events were found (Figure 5), with the occurrence of one or more events in 74% of the years, for this period. The years of 2007 and 2014 were particularly extreme and should be highlighted due to the amount of reported events and their severity (Figure 6), which resulted in relevant economic losses (Â. Santos et al., 2014).

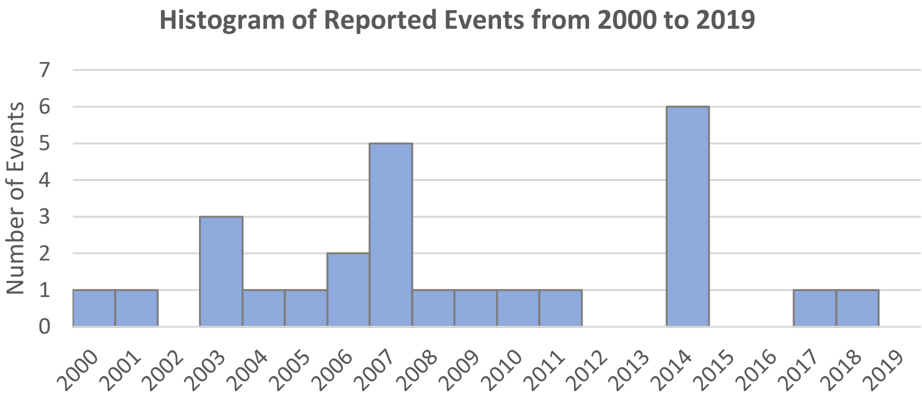

Figure 5. Histogram of documented events of extreme oceanographic conditions where wave overtopping, flooding or beach erosion occurred, between 2000 and 2019 for Costa da Caparica urban beaches.

Figure 6. Examples of events at the coastal front of Costa da Caparica. Left panel, newspaper clipping from Diário de Notícias in January 2014. Right panel, photo published by Público newspaper in January 2014.

2.2. Characterization of the hydrodynamic conditions

2.2.1. Southern Portuguese coast

The wave climate at the southern coastal sites of Praia de Faro and Quarteira was computed from data between January 1993 and November 2019 extracted from the "Faro Costeira" buoy, located at depths of 93 m (https://www.hidrografico.pt/). The significant wave height (Hs) displays a clear seasonality with higher wave heights in winter and lower heights in summer (Figure 7). Similarly, the peak period exhibits a seasonal behaviour. Waves from the SW direction are approximately 75%, while the SE waves represent around 25%. The average Hs and Tp values are 1.1 m and 8.4 s, respectively. The study area is mesotidal with a mean tidal range of 2.8 m during spring tides and 1.3 m during neap tides, with a maximum tidal range of 3.5 m and a mean tidal range of 2.1 m (Almeida *et al.*, 2012). Storms are characterised by Hs > 2.5 m, according to Almeida *et al.* (2012).

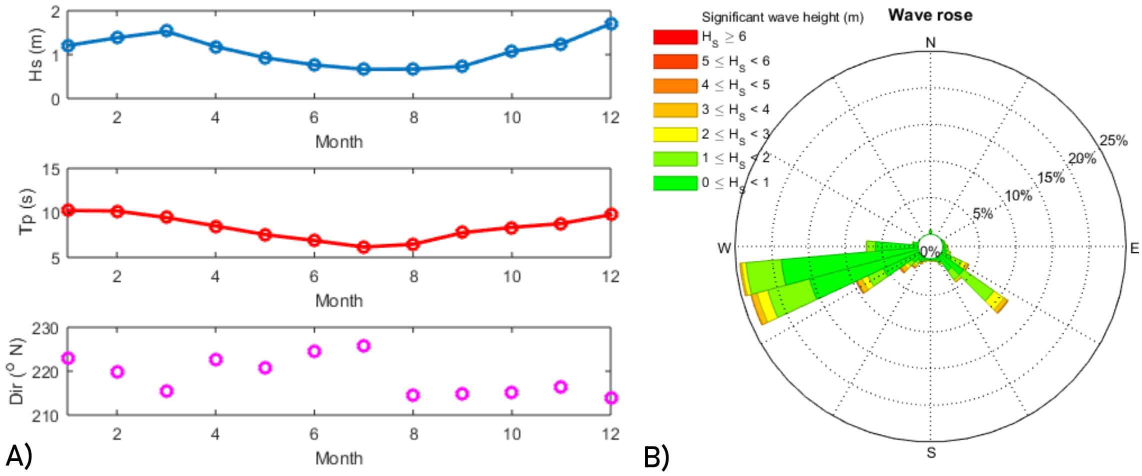

Figure 7. A) Mean of Hs per month (upper panel), associated mean Tp (middle panel) and Dir (lower panel). B) Wave rose for Hs at "Faro Costeira" buoy (1993- November 2019).

Previous authors observed an evident positive correlation between Hs and storm surge for stormy wave conditions from SW events (> 180°) (Rodrigues *et al.*, 2012). This trend was not found when eastern (SE, < 180°) wave conditions were considered. In this report, the information has been updated and it covers until November of 2019, for both wave directions (Figure 8). The storm surge and Hs observed during SW events are clearly larger than those reported during SE events. The surge observations were extracted from Huelva tidal gauge.

Rodrigues *et al.* (2012) also proposed a linear relation between Hs and Tp for SW events. In this report, a different methodology was applied to obtain an equation relating Hs and Tp (Figure 9), for both quadrants and updated to November 2019. Thus, the adopted methodology splits the dataset between SE and SW directions. Hs is grouped in cells of 0.5 m (i.e., between 1.5 and 2.0 m, 2.0 and 2.5 m, etc.). Then, Hs mode is calculated for each cell and for the corresponding Tp values. Finally, a power equation is adjusted to the mode values. The statistical parameters shown in Figure 9 evaluate the goodness of fit of the power equation in relation to the mode values. In general, the adjustment for the two cases is good. When evaluating the entire dataset, the root-mean-square error (RMSE) is larger for SW conditions (RMSE=4.0 s) than for SE conditions (RMSE=0.87 s). This is mainly due to the significant scatter observed for the cases with Hs < 3 m. For Hs > 4 m, the scatter is clearly lower.

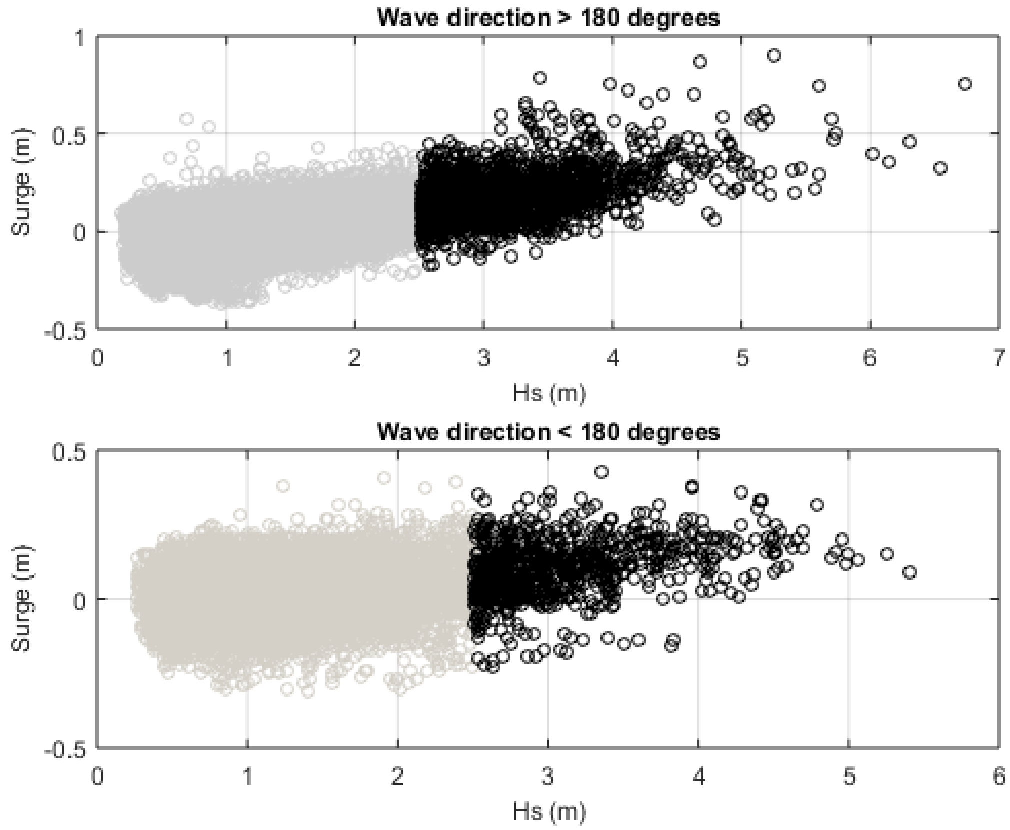

Figure 8. Scatter plot of Hs against surge for the two dominant wave directions at the southern Portuguese coast. Grey dots represent non-storm events and black dots display storm events according to Almeida et al. (2012).

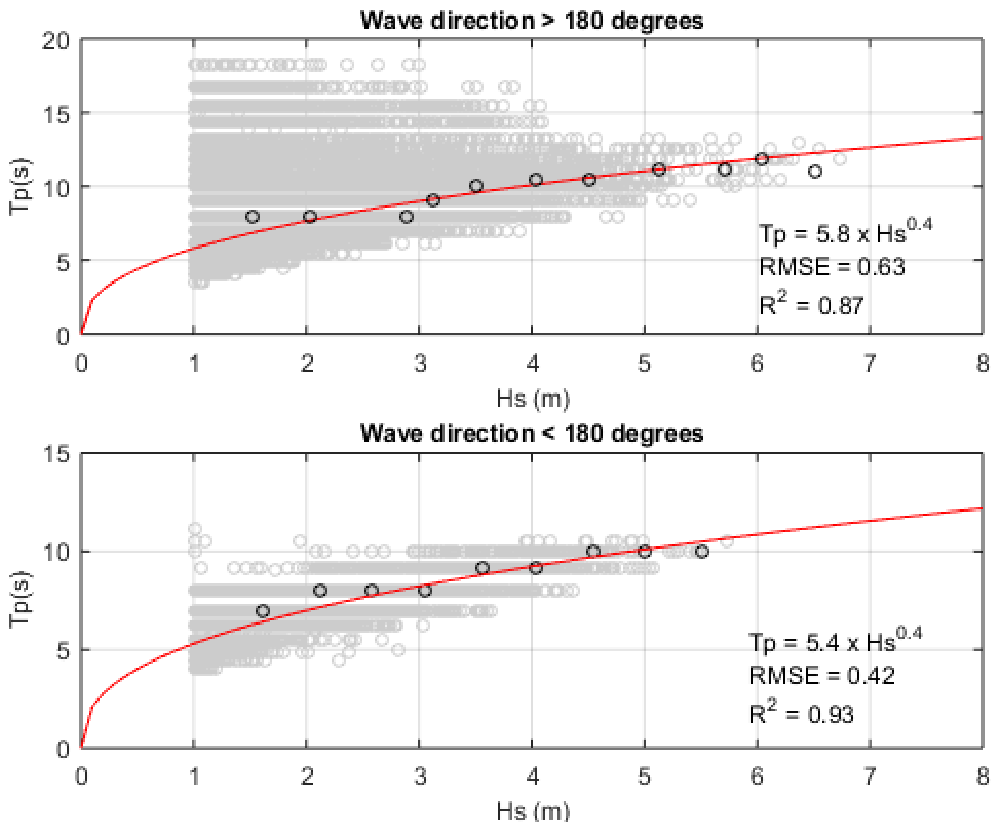

Figure 9. Scatter plot of Hs against Tp for the two dominant wave directions at the southern Portuguese coast. The red line indicates the fit line and the black dots indicate the mode value calculated after grouping Hs every 0.5 m.

2.2.2. Costa da Caparica

The western coast of mainland Portugal is characterised by the predominance of northwest waves (Costa *et al.*, 2001). However, extreme events (storms) occur in two distinct directions in this region of the Atlantic. According to Rogers (1997), extratropical storms coming from northwest may occur, in line with the main regime of wave climate, but also subtropical storms from southwest can be observed. According to Costa *et al.* (2001), the maritime storms on the west coast correspond to offshore significant wave heights Hs ≥ 4.5 m.

The nearest equipment with available wave measurements in the study area is the Lisbon Port Authority coastal buoy (APL buoy), positioned at the entrance of the southern channel from the inlet of the Tagus estuary (M = -109 278.6 m; P = -114 962.7 m, coordinate system: PT-TM06/ETRS89) (http://www.portodelisboa.pt/), at the -22 m ZH bathymetric, with ZH the chart datum and MSL=+2.00 m ZH. While there are not enough continuous records from this equipment to characterise adequately the wave climate in the study area, these data were used to validate wave propagation from offshore to nearshore (at the same water depth).

Wave propagation was performed with the numeric model SWAN (*Simulating WAves Nearshore*) (Booij *et al.*, 1999). Global model WAM (*ECMWF - European Centre for Medium-Range Weather Forecasts*) was used to obtain the offshore wave dataset, between 2008 and 2018, from two offshore locations, named as Input_1 and Input_2 (Figure 10), respectively. These two datasets of offshore data were considered regarding to the storm regimes and the exposure of the coastal section under study. The first one, Input_1, was imposed on all the northern boundary and the second one, Input_2, on the southern and western boundaries of the regional computational domain.

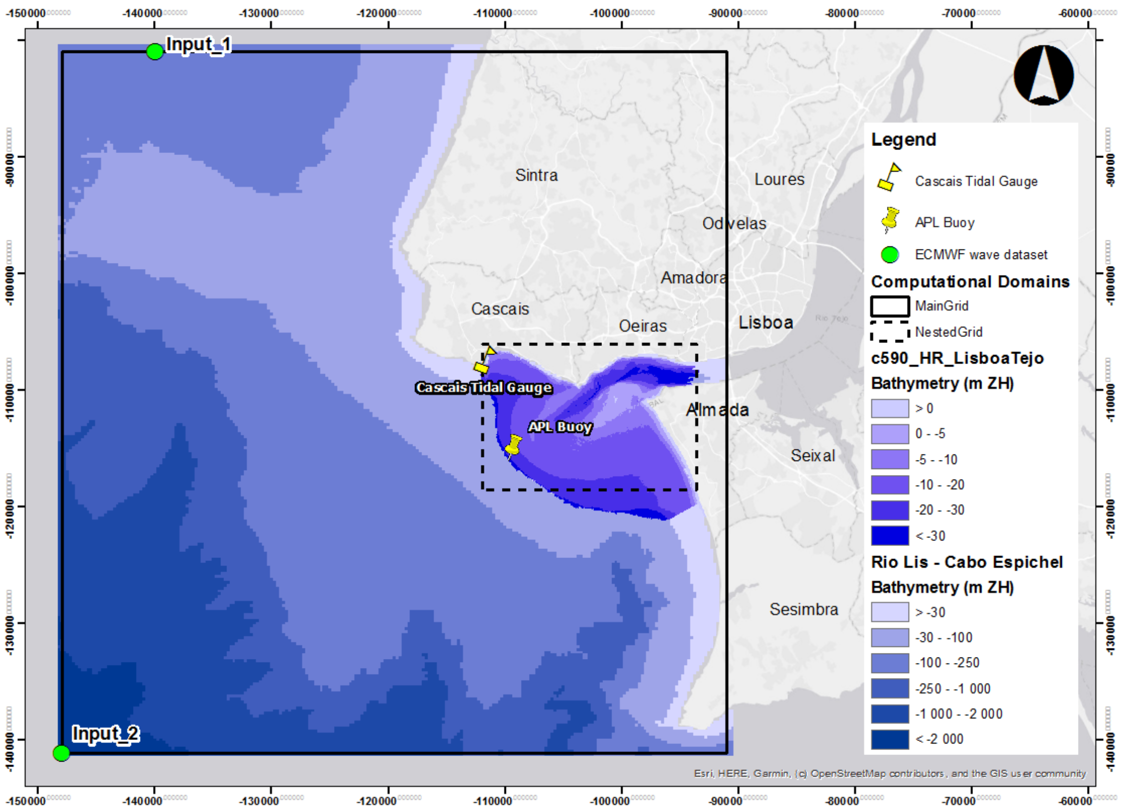

Figure 10. Representation of bathymetry and computational domains used in the SWAN model. Points where the ECMWF wave dataset were obtained (Input_1 and Input_2). Locations of APL buoy and Cascais tide gauge.

Wave climate characterisation was performed at the APL buoy location, named as Point APL Buoy, which was assumed as representative of the local wave climate, with SWAN results. At this location, of intermediate water depths, it is assumed that storm conditions are related with Hs > 4 m, and not 4.5 m as in deep waters (mentioned above).

The wave climate in this region is markedly seasonal (Figure 11), with the highest and longer waves occurring during the maritime winter, from October to March, and with the less energetic wave climate during the maritime summer, from April to September. The average monthly regime is characterised by the mean of the maximum Hs for each month and the related peak period and wave direction, Tp and Dir, respectively. For the average monthly regime, Hs > 4 m between December and February. The associated Tp values reveal that the higher periods occur between October and March, with values around 14 s. The associated wave directions are more rotated south in the maritime winter than during the maritime summer.

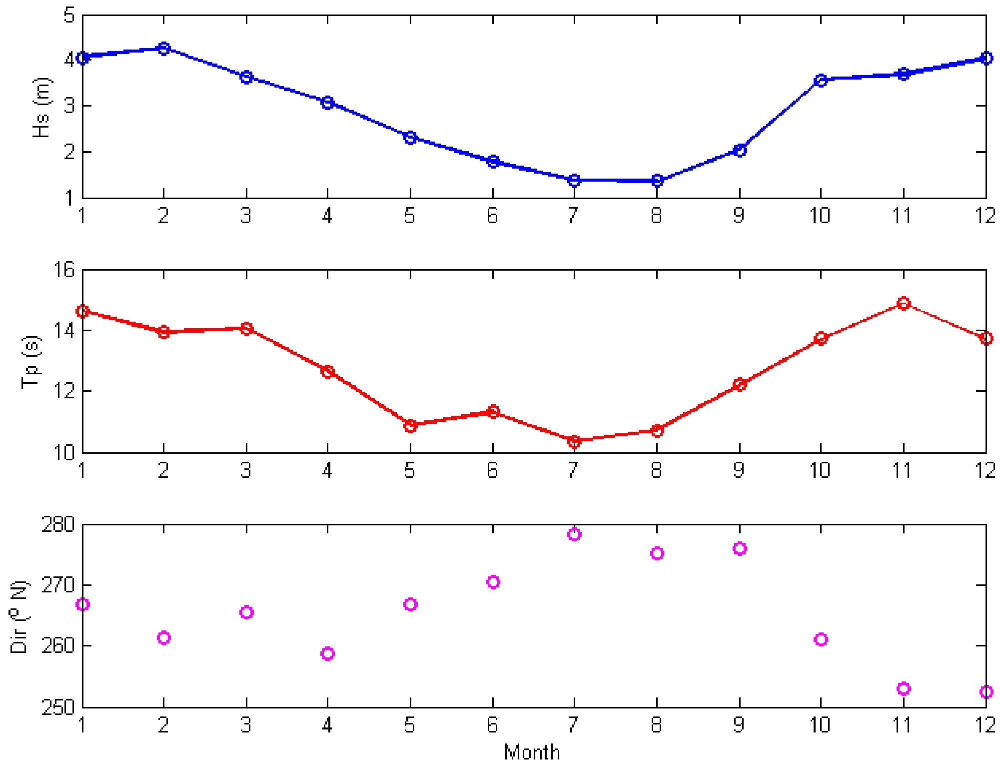

Figure 11. Wave regime obtained from 2008 to 2018 at Point APL Buoy. Mean of Hs maximums per month (upper panel), associated mean Tp (middle panel) and Dir (lower panel).

The seasonal analysis at Point APL Buoy (Figure 12, left panel) shows that the longer periods occur in the maritime winter and can exceed 20 s. Although the highest values of Hs can be associated to Tp values in the order of 15 s, for Hs ≥ 4 m, the associated Tp range from about 9 s up to 20 s. The regional wave climate shows a slight rotation to the south in the maritime winter (Figure 12, right panel, and Figure 13), with more occurrences coming from the west, mainly relevant for higher Hs values, even though the wave direction dominance remains from WNW. For Hs ≥ 4 m, waves arrive predominantly from the west, with some occurrences from WSW, which is characteristic of subtropical storms.

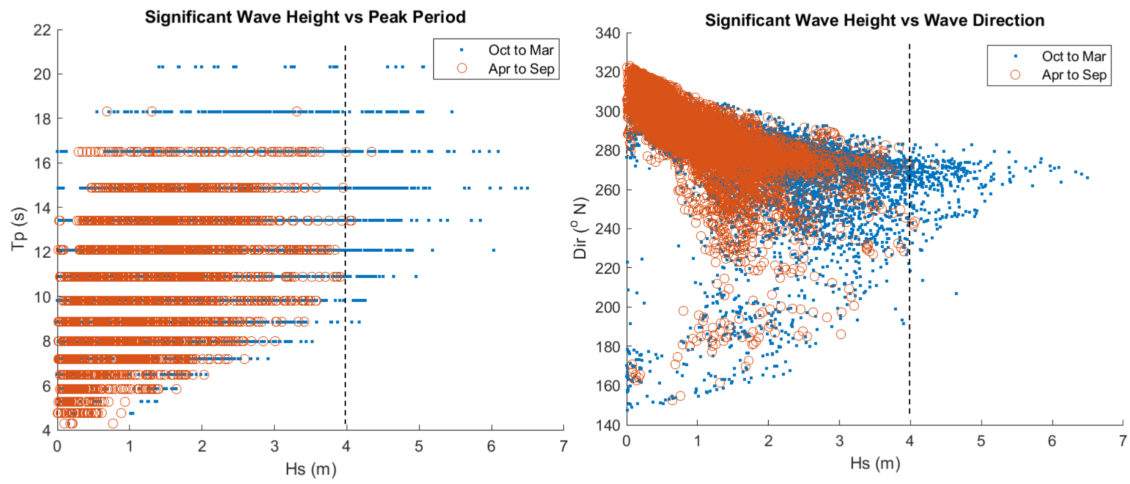

Figure 12. Seasonal analysis of characteristic wave parameters at Point APL Buoy. Distribution of peak period as a function of significant wave height (left panel). Distribution of wave direction as a function of significant wave height (right panel).

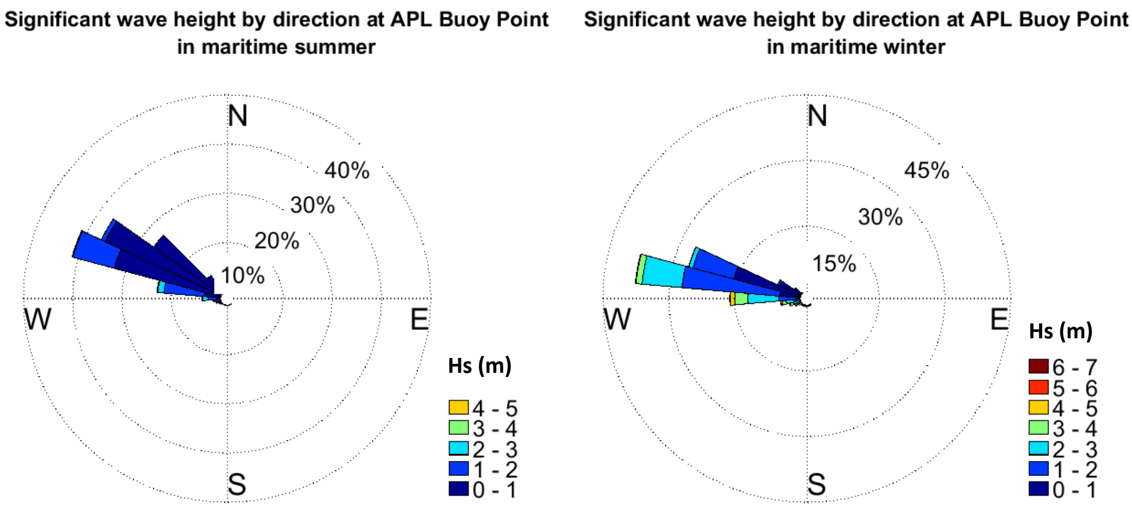

Figure 13. Directional distribution of significant wave heights at Point APL Buoy for the maritime summer, between April and September (left panel), and for the maritime winter, from October to March (right panel).

It should be noted that, at Point APL Buoy, waves from the NW quadrant already suffered diffraction caused by the Lisbon Peninsula, rotating west, which tends to be perpendicular to the case study coastline (Figure 13).

Overall, between 2008 and 2018, the average values of Hs and Tp were 1.19 m and 11.2 s, respectively, at the Point APL Buoy, with higher energetic waves during the maritime winter (average values of Hs and Tp of 1.62 m and 12.6 s, respectively). The average monthly values of Hs and Tp increase up to 2.93 m and 12.72 s, respectively, with the maximum values being measured in the maritime winter, with Hs = 6.50 m and Tp = 20.3 s.

Caparica astronomic tidal regime is semi-diurnal, with mesotidal amplitude. Based on Cascais tidal gauge data between 1990 and 2000, Taborda *et al.* (2010) obtained main tidal characteristics, as shown in Table 1.

Table 1. Astronomic tide levels (m MSL) based on Cascais tidal gauge data from 1990 to 2000 (Taborda et al., 2010).

HTmax	HTsp	HTmean	HTnp	HTmin	LTmax	LTnp	LTmean	LTsp	LTmin
1.95	1.53	1.18	0.81	0.48	-0.23	-0.56	-0.93	-1.27	-1.62

(Legend: HT – High Tide; LT – Low Tide; max – maximum; mean – average; min – minimum; sp – spring; np – neap)

2.3. Field surveys

The results of this report are based on field surveys carried out within the scope of the EW-Coast project, as well as on surveys performed by other entities / projects, when available. To this end, the available data were gathered. The performed fieldwork included topographic surveys and collection of sediment samples for grain size analysis.

2.3.1. Sedimentology

2.3.1.1. Quarteira

In May 28, 2019, 9 sediment samples were collected at Quarteira. The samples were equally distributed along the three beaches, with one located at the upper part of the profile (upper berm), one near the berm crest and another in the lower part of the profile, at the beach face. These samples were processed with the software GRADISTAT (Blott and Pye, 2001). The 99% of the sediment is classified as sand, and 1% as gravel. The mean grain size (D) is 485 µm and d90 is 900 µm. The sediment fall velocity, w_s, is directly related with D. According to the expressions proposed by Van Rijn (1993), w_s can be calculated as follows (Eq. (1)):

$$w_s = \frac{\Delta\, g\, D^2}{18\, \nu}; \qquad 1 < D \leq 100\ \mu m$$
$$w_s = \frac{10\, \nu}{D}\left[\left(1 + \frac{0.01\, \Delta\, g\, D^3}{\nu^2}\right)^{0.5} - 1\right]; \qquad 100 < D < 1000\ \mu m \qquad \text{Eq. (1)}$$
$$w_s = 1.1\, (\Delta\, g\, D)^{0.5}; \qquad D \geq 1000\ \mu m$$

where g is the standard acceleration due to gravity, Δ is the relative density of the sediment and ν is the kinematic viscosity. The value of w_s calculated for Quarteira is 0.07 m/s.

2.3.1.2. Faro

No sediment samples were collected at this site and values reported in the literature (Vousdoukas *et al.*, 2012b) were used to calculate the sediment fall velocity. Using D=500 µm, according to Eq. (1), the sediment fall velocity in Praia de Faro is w_s=0.07 m/s.

2.3.1.3. Costa da Caparica

Two sediment surveys were carried out at Caparica: in May 30, 2019, with nine collected samples; and in October 18, 2019, with eight collected samples. In each survey, sediments were sampled from the low-tide terrace, the beach face and the berm of three central beaches, namely Santo António, CDS and Traquínio-Paraíso beaches. These samples were processed with the software GRADISTAT (Blott and Pye, 2001).

The results show that all samples are unimodal, with the May samples being classified as fine to medium sand, moderately well sorted to very well sorted, where the coarser sand and less sorted was found at CDS beach. However, in October, all samples were classified as medium sand, being moderately well sorted to well sorted. The samples from the low-tide terrace presented a higher heterogeneity.

The grain size showed small variation (Table 2), with the major differences recorded between surveys, which is reflected on the sediment fall velocity.

Table 2. Characteristic grain sizes (D and d_{90}) and sediment fall velocity (w_s) for sediment samples collected in May 30 and October 18, 2019 at Costa da Caparica.

	30/05/2019			18/10/2019		
	Minimum	Maximum	Average	Minimum	Maximum	Average
D (μm)	190	333	245	328	500	383
d_{90} (μm)	243	501	365	495	687	580
w_s ($m.s^{-1}$)	0.02	0.05	0.03	0.05	0.07	0.06

2.3.2. Topography

2.3.2.1. Southern Portuguese coast

Researchers from the Centre for Marine and Environmental Research (CIMA) of the University of Algarve (UAlg) (https://www.cima.ualg.pt/) have been conducting periodic surveys along Praia de Faro during the last years. In this report, the authors focus on four profiles measured in 2018 and 2019. On the other hand, Quarteira has only been surveyed three times, in 2019, as shown in Table 3. The profile elevation was measured with a digital GPS with recorded information every 25 cm. The Hs values reported during the period of the field surveys, 2018 and 2019, are illustrated in Figure 14.

During January 2018, only one storm event was reported. The first field campaign took place at Praia de Faro on February 26, 2018, 27 days after the previous storm and two days before the second event. This event, storm Emma, was a very severe storm with Hs up to 6.5 m, equivalent to a 16-year return period event (Ferreira *et al.*, 2019). The impact of storm Emma was measured with the data collected during the second survey, in March 2, 2018. After this event, a few storms hit the area with Hs reaching up to 4.5 m. The third field survey occurred on April 20, 2018, one month after storm Emma. The wave conditions were very calm during the rest of 2018, with only one moderate event (Hs > 4 m) in November, a month after the fourth survey (October 12, 2018). The wave conditions during the winter and spring of 2019 were not especially highly energetic. The next field survey was carried out on May 28, 2019, two months after the last event. During the next months (including October 2019, when the next field campaign was performed), the wave conditions were very calm. In the second half of December 2019, two events hit the area: Daniel storm, in December 14-15, 2019; and Elsa storm, in December 19-20, 2019. Hs reached up to 3.9 m and 5.2 m, respectively. Thus, two field campaigns were carried out on December 17 and 20, 2019, to measure the impact of these storms in the sites.

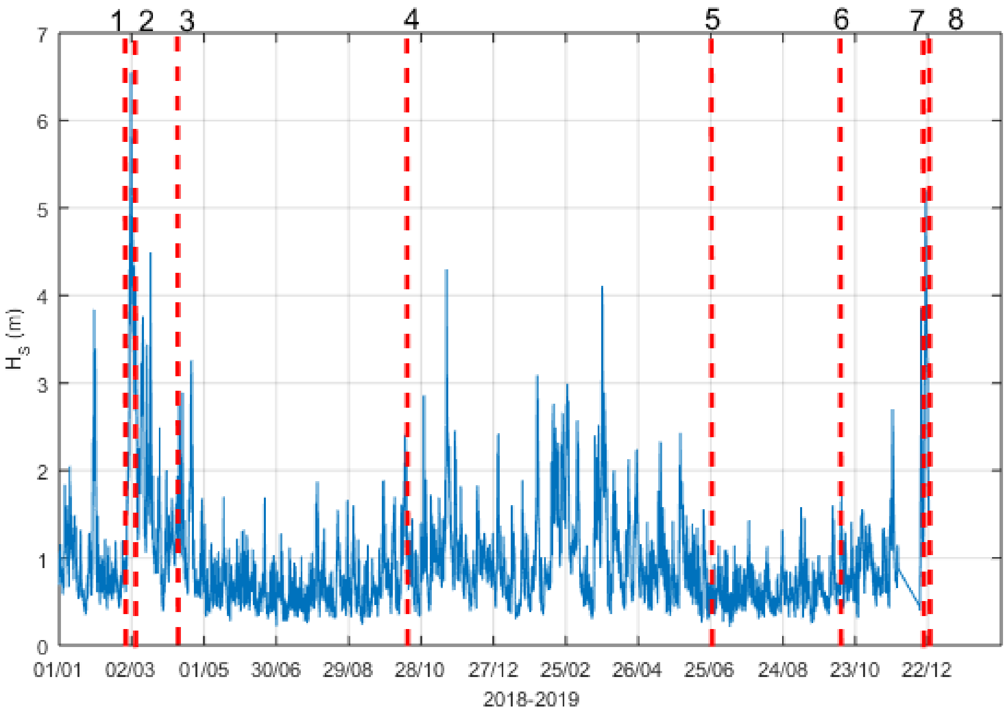

Figure 14. Significant wave height measured in 2018 and 2019. The data extracted from the buoy reaches only until November 2019, and the last month information was completed with data provided by forecast products from Puertos del Estado (https://www.puertos.es/). The dashed lines represent the field campaign dates and the numbers refer to the surveys ID (Table 3).

Table 3. Dates of the field surveys and sites visited.

ID	Date	Site
1	26/02/2018	Praia de Faro
2	02/03/2018	Praia de Faro
3	20/04/2018	Praia de Faro
4	12/10/2018	Praia de Faro
5	28/05/2019	Quarteira
6	02/10/2019	Praia de Faro
7	17/12/2019	Quarteira
8	20/12/2019	Quarteira / Praia de Faro

2.3.2.1.1. Quarteira

Three topographical surveys were performed at the study site of Quarteira in 2019. The first one was conducted by an unmanned aerial vehicle (UAV) and it was carried out in May 28, 2019 (see Table 3). A Digital Elevation Model (DEM) of the study area was created with less than 5 cm resolution. Then, two consecutive walking DGPS-GNSS topographical surveys were performed along nine profiles (three in each beach), as shown in Figure 15. These surveys were made on December 17, 2019, after Daniel storm and before Elsa storm, and in December 20, 2019, after Elsa storm.

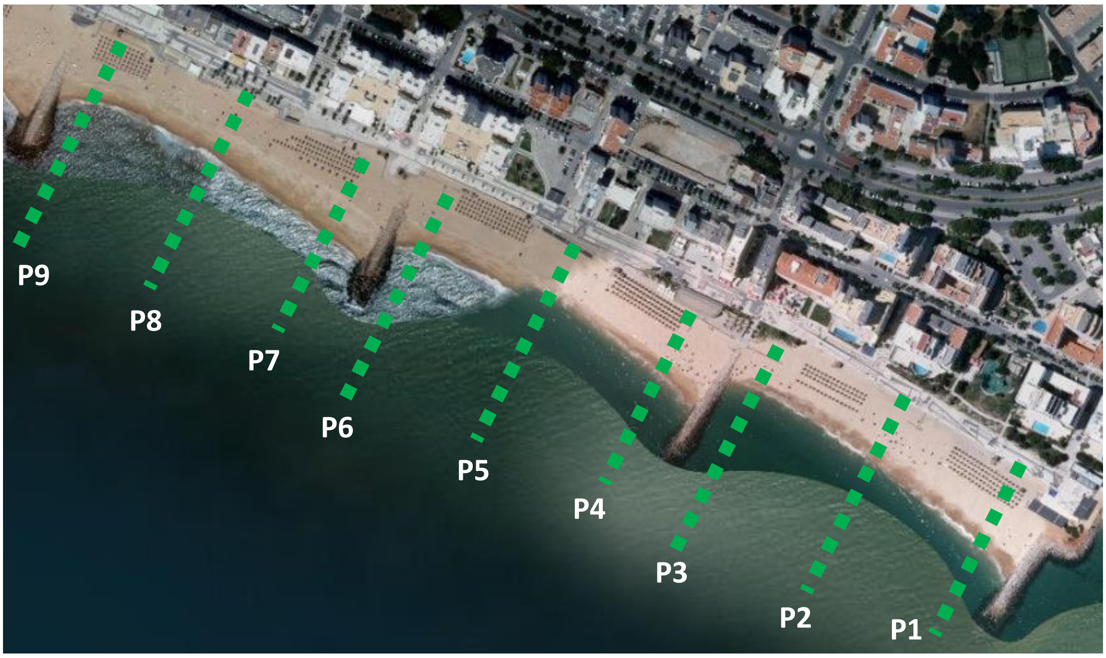

Figure 15. Location of the 9 profiles analysed in Quarteira. Source: Esri, DigitalGlobe, Geoeye, Earthstar Geographics.

During the May 2019 survey, Quarteira beaches were easterly rotated as the result of the dominant western wave conditions. However, some accumulation, although less significant, was also observed downdrift, in relation to the groins (Figure 16).

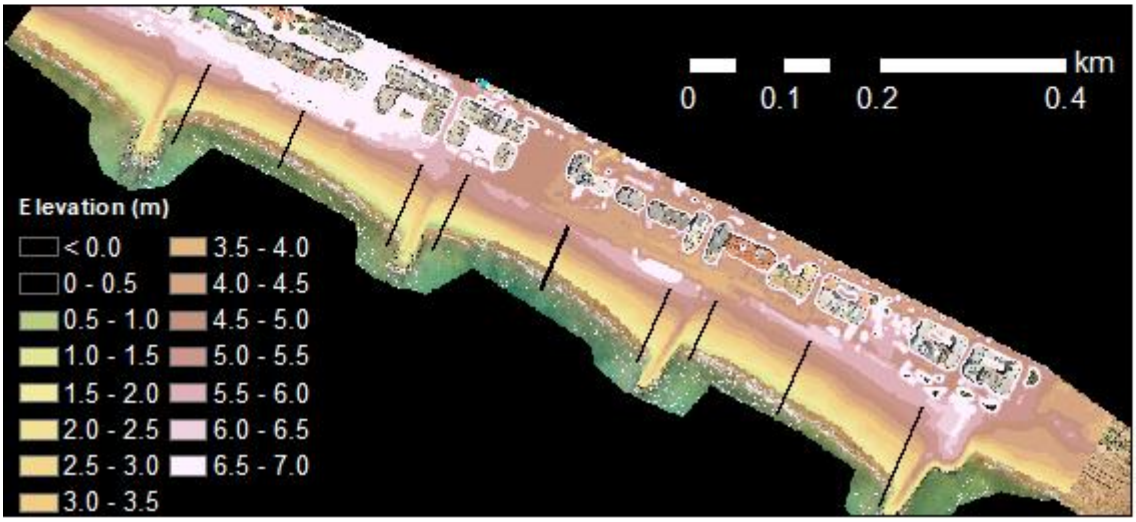

Figure 16. Morphologic representation of Quarteira site obtained during the survey of May 2019. Elevation referred to MSL. Black lines represent the topographic profiles (P1 to P9 from SE to NW).

Under the dominant western wave conditions, the width of each beach displays an alongshore variable length, with the largest width close to the eastern groin, a reduction when moving towards NW (the shortest width approximately in the central part) and another increase in the most extreme western section. In each beach, the western groin produces a shadow area immediately behind, and locally orienting the alongshore currents within the shadow area from SE to NW, and transporting the sediment in the same direction. Outside the shadow area, the wave angle causes an alongshore current from NW to SE, accumulating sediment updrift of the groins.

Regarding the profile morphology, profiles P1, P6 and P7 were wider and P1, P4 and P7 exhibited gentler slopes, while the rest of the profiles displayed a steeper slope (Figure 17). For instance, P7 had a slope of approximately 0.06, the slope of P8 was 0.10 and P9 had a 0.11 slope (Table 4). The slope was estimated between the lower portion of the profile and 4 m above MSL, where the berm was found in December 2019 surveys; the position of the berm was not well defined in the survey of May 2019. In this survey, it is also important to highlight the absence of a well-developed berm step and the berm does not exhibit a flat surface, making the transition between the berm and the beach face very smooth. For the dominant conditions (Figure 7), Quarteira beaches can be defined as reflective, according to Masselink and Short (1993). However, the measurements taken in December 20, 2019 suggest that the beaches were not fully recovered from the previous events and their states can be generically classified as intermediate barred (Figure 1).

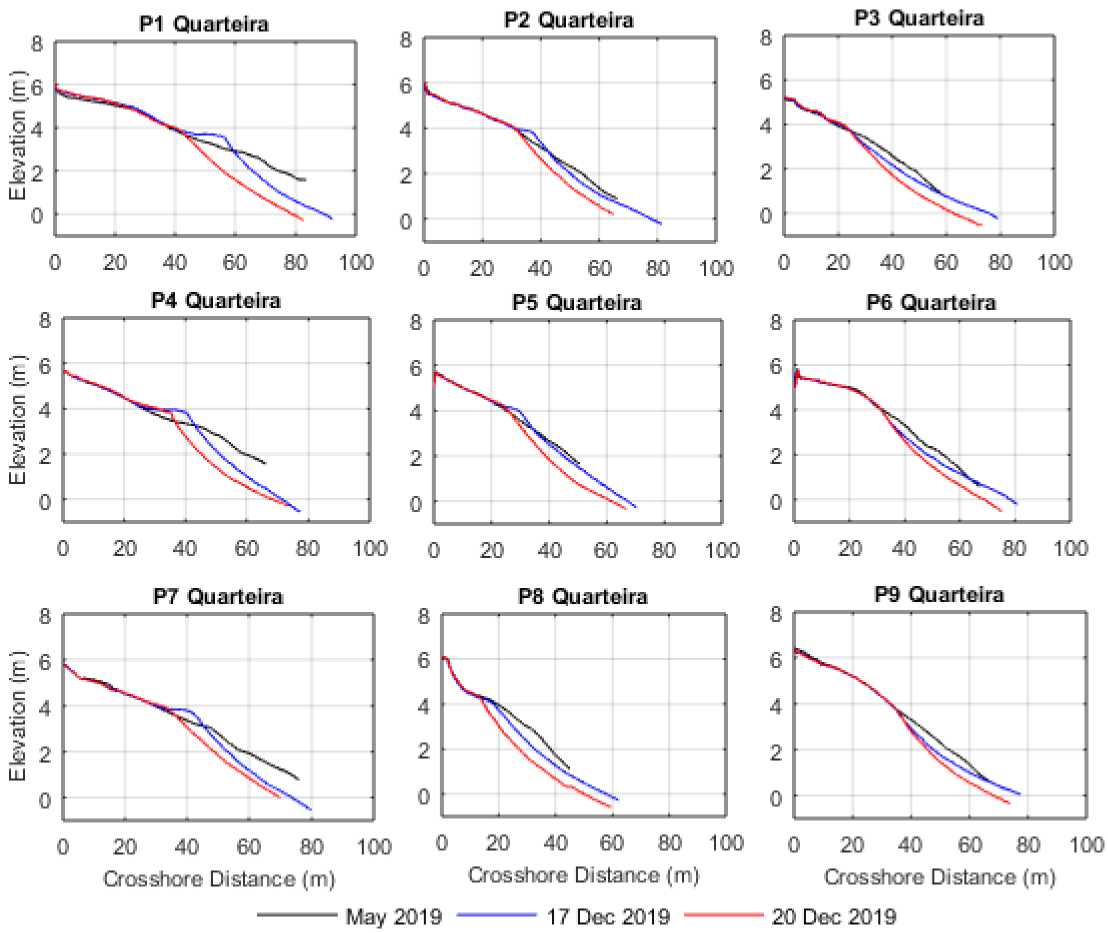

Figure 17. Topographical profiles obtained at Quarteira during the 2019 surveys. Elevation referred to MSL.

Table 4. Berm width, beach face slope and beach state at Quarteira site.

28/05/2019									
	P1	P2	P3	P4	P5	P6	P7	P8	P9
Berm (m)	65	26	28	52	24	25	45	17	23
Slope	0.06	0.09	0.08	0.06	0.09	0.10	0.06	0.10	0.11
Beach state	Pre-storm conditions/ Reflective (no well-marked berm)								

17/12/2019									
	P1	P2	P3	P4	P5	P6	P7	P8	P9
Berm (m)	55	36	23	40	28	30	41	17	34
Slope	0.11	0.11	0.08	0.12	0.10	0.08	0.11	0.10	0.09
Beach state	Pre-storm conditions/ Reflective (well-marked berm)								

20/12/2019									
	P1	P2	P3	P4	P5	P6	P7	P8	P9
Berm (m)	41	31	23	35	24	30	33	13	34
Slope	0.10	0.13	0.09	0.11	0.11	0.10	0.10	0.11	0.11
Beach state	Post-storm conditions / Intermediate barred (well-marked berm)								

The second survey, on December 17, 2019, after the impact of the first storm, showed that the beach continued easterly rotated with the largest beach width in P1, P4 and P7. Also, the berm was more developed in those profiles and it reduced its importance when moving westerly. Likely, that was caused by the storm that eroded more these regions of the three beaches. The berm width ranged between 55 m (P1) and 40 m (P4) at the eastern section of the beaches, between 36 m (P2) and 17 m (P8) at the central part and between 34 m (P3) and 23 m (P6) at the western sections (Table 4). The beach face slope, calculated from the lowest point of the profile to the berm, was steeper at the eastern sections and gentler at the western sections. For instance, P7, P8 and P9 had slopes of 0.11, 0.10 and 0.09, respectively. Regarding the profile evolution between May and December 17, 2019, the beaches were more intensively eroded in their eastern parts (P1, P4 and P7), while P3, P6 and P9 displayed a less severe change.

The next survey was carried out on December 20, 2019, after the storm Elsa. This event eroded a large part of the berm, especially in the eastern side of the beaches. The berm retreated up to 14 m (P1). The beach face slope exhibited comparable values to the previous survey: generally, 0.10 - 0.11 for the profiles located at the central and eastern regions of the beaches (P1, P4, P5, P7, P8), while P3 and P6 showed a steeper profile (P9 had a similar slope to those of P7 and P8). As it was observed in the previous survey, the storm impacted more intensively in the eastern sections of the beaches and higher volumes of sediment were removed from P1, P4 and P7 than P3, P6 and P9. The authors hypothesize that the higher erosion observed at the eastern sections of the beaches may be caused by higher exposure to wave action and higher degree of readjustment to an after-storm profile, increasing the cross-shore sediment transfer. After this event the beach could be classified as an intermediate barred beach.

From the obtained data it is possible to observe three different beach conditions, from a wider (but not well-defined) berm in May 2020 to a smaller (eroded) berm after the two storms. The beach face slope did not display a large variation between the surveys conducted on December 17 and 20, 2019.

2.3.2.1.2. Faro

Four profiles were surveyed in 2018 and 2019 at Praia de Faro. The location of these profiles is shown in Figure 18.

The survey performed in February 2018 displayed a well-developed berm in the eastern part of the study area, with widths of 20 m and 26 m at profiles P1 and P2, respectively, as illustrated in Figure 19. The beach face slope of the profiles ranged between 0.13 and 0.14 (Table 5). The beach state can be classified as reflective.

The storm impact was very significant in the four profiles and the vertical erosion was up to 2 m, with the berms being completely eroded. Also, the beach adapted to the very energetic conditions and the beach slope became more dissipative with the slope varying between 0.06 and 0.08. Moreover, visual inspections revealed the existence of a submerged sandbar. Due to the storm, the beach transitioned from reflective to an intermediate beach state, probably an intermediate barred according to Masselink and Short (1993) classification. The sediment volume began to recover immediately after Emma (not shown here), observed at the post-storm survey, 6 days after the storm hit the site.

Figure 18. Location of the four profiles monitored in Praia de Faro. Source: Esri, DigitalGlobe, Geoeye, Earthstar Geographics.

In the survey conducted on April 20, 2018, the average sediment gain was 81% of the total loss, especially in the low beach face, while the sediment did not refill the upper part of the profile. The berm was again observed, although for P1 and P2 it was not as well-developed as it was in February, and for P4 it developed further. The beach face slope increased considerably with respect to the previous survey and it ranged between 0.10 and 0.15. Visual observations at Praia de Faro revealed that some sediment was forming submerged longshore bars.

In the next survey, conducted in October 12, 2018, the profiles did not experience large variations in relation to the previous survey, and there was still a lack of sediment in the upper part of the profile. Furthermore, topographical data extracted from the COSMO program (COSMO, n.d.) displayed upper beach-face cusps (Figure 20).

Low energetic conditions in the summer and fall of 2019 preceded the next survey, performed in October 20, 2019. In this survey, the profiles were similar to those of the previous year.

However, some material reached again the upper part of the profile. The beach face slope varied between 0.12 and 0.14.

The last survey was carried out in December 20, 2019, after the impact of two consecutive storms. They caused some erosion in respect to the profile measured in October 2019, with vertical differences of up to 1 m. Also, the beach face slope slightly reduced and varied between 0.10 and 0.13. A well-developed berm was only observed at P1.

Thus, a pre-storm profile would be similar to the February 2018, April 2018, October 2018 and October 2019 surveys, while a highly eroded profile (post-storm or sequence of storms) would be similar to the survey carried out in March 2018, as highlighted in Table 5.

Table 5. Berm width, beach face slope and beach state at Praia de Faro. (-) represents no berm, no profile surveyed or incomplete profile (for slope determination).

	26/02/2018			
	P1	P2	P3	P4
Berm (m)	20	26	11	10
Slope	0.14	-	0.13	0.14
Beach state	Pre-storm conditions/ Reflective			

	02/03/2018			
	P1	P2	P3	P4
Berm (m)	-	-	-	-
Slope	0.07	0.07	0.08	0.06
Beach state	Post-storm conditions / Interm. barred			

	20/04/2018			
	P1	P2	P3	P4
Berm (m)	19	21	11	15
Slope	0.13	0.10	0.15	0.15
Beach state	Pre-storm conditions/ Reflective			

	12/10/2018			
	P1	P2	P3	P4
Berm (m)	17	-	10	12
Slope	0.13	-	0.13	0.13
Beach state	Pre-storm conditions/ Reflective			

	20/10/2019			
	P1	P2	P3	P4
Berm (m)	11	25	15	10
Slope	0.12	0.12	0.14	0.12
Beach state	Pre-storm conditions/ Reflective			

	20/12/2019			
	P1	P2	P3	P4
Berm (m)	10	-	-	-
Slope	0.11	-	0.13	0.10
Beach state	Post-storm conditions / Interm. barred to reflective			

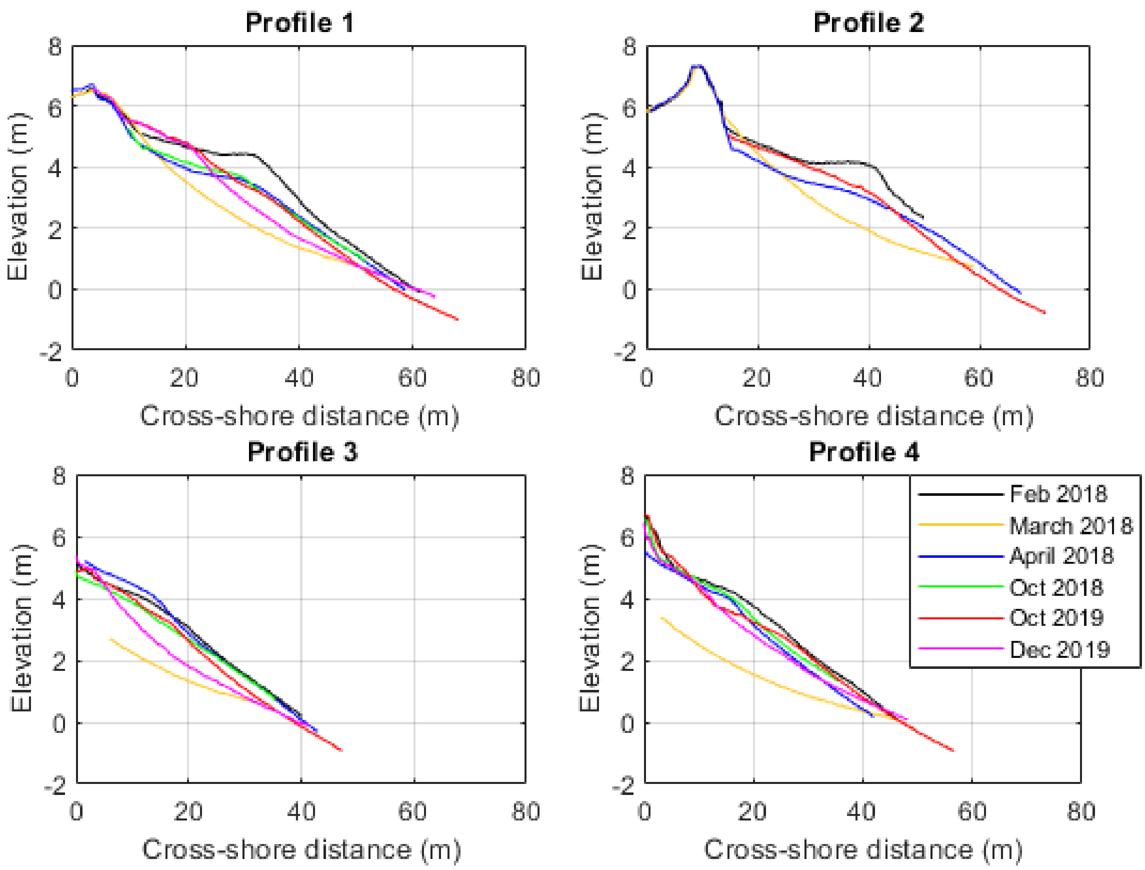

Figure 19. Topographical measurements taken at Praia de Faro during the survey period of 2018-2019. Elevation referred to MSL.

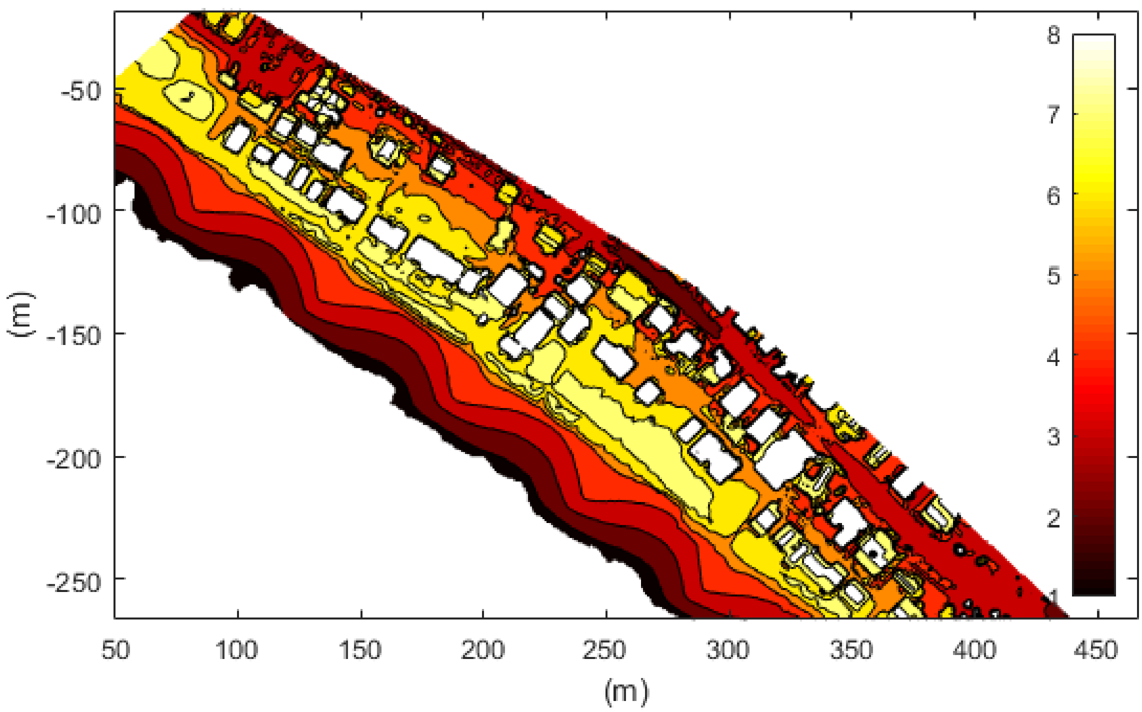

Figure 20. Beach topography extracted from the COSMO program (COSMO, n.d.). Elevation referred to MSL. The survey was conducted in October 2018.

2.3.2.2. Costa da Caparica

Within the scope of the EW-Coast project, two surveys were carried out at Costa da Caparica site, in May and October 2019. Since other surveys were performed by several institutions for multiple projects, a search of the available data was made. Two further data sets were collected: from the COSMO program (https://cosmo.apambiente.pt/); and from the Municipality of Almada, resulting from a partnership protocol between the Municipality of Almada and the Dom Luiz Institute / FCUL Geology Centre. The selected profiles included in this report are shown in Figure 21.

In addition to these data, beach state indicators (beach face slope, beach surface area and beach volume; see Figure 22), resulting from surveys carried out between 2011 and 2013 at Costa da Caparica, are available in the literature (Diogo *et al.*, 2013).

In order to compare results, these indicators were obtained for all available surveys, using the methodology described by Diogo *et al.* (2013):

- Beach Volume per unit of coast length, in m^3/m - calculated between the terrestrial limit of the beach and the MSL; numerically and dimensionally equal to the section area limited by the profile;
- Beach surface per unit of coast length, in m^2/m - projected horizontal distance calculated between the terrestrial limit of the beach and the level of 2.5 m above MSL per unit of coast length; numerically and dimensionally equal to the projected horizontal distance between the profile limits;
- Beach face slope, m/m, equal to tan β - calculated between the levels of 1 and 2 m above MSL.

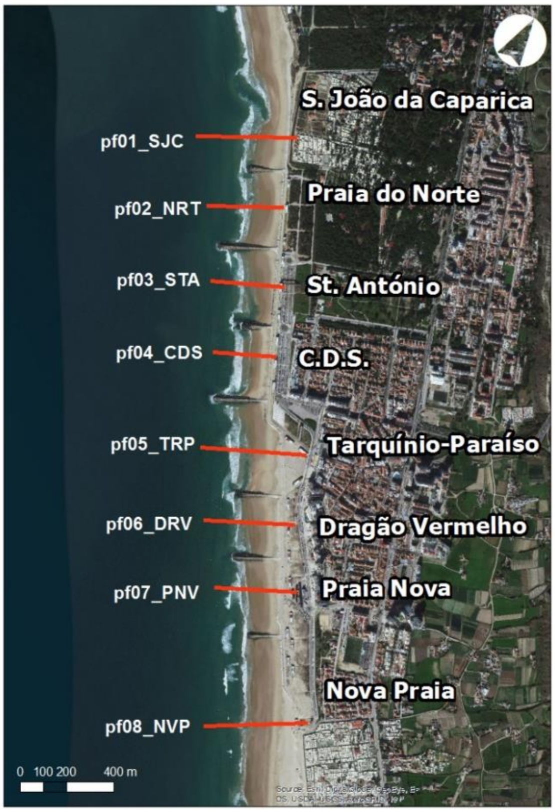

Figure 21. Location of the profiles surveyed in Costa da Caparica and names of the beaches (Source: Esri, DigitalGlobe, GeoEys, Earthstar Geogrphics, CNES/Airbus Ds, UsDA, UsGs, AeroGrid, IGN and GIS User Community).

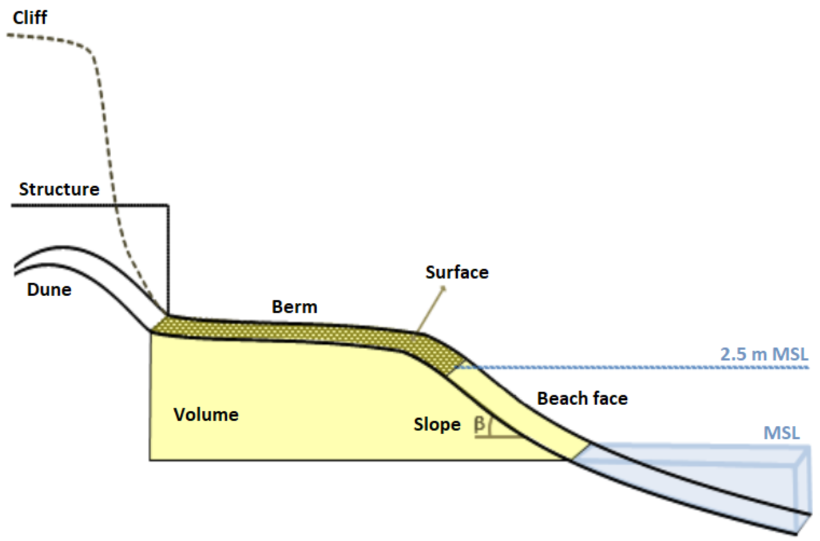

Figure 22. Representation of the morphological approach to calculate for each beach profile: volume, surface and beach face slope (Diogo et al., 2013).

All results are presented in attachment (see Annex I). In some cases, beach profile indicators could not be calculated because the profile did not fit the methodology calculation conditions described above, being a limitation of the methodology. Time and space analyses were performed, for all indicators, and confronted with extreme events and with beach nourishments.

The beach cells, created by the coastal defences, are very narrow. During high tides, it is quite common that the swash zone reaches the structure. In these cases, there is no room for the formation of berms in the beach profile. The beach surface indicator may reflect the development or absence of berm formation, as well as beach carrying capacity for recreational purposes (Carapuço *et al.*, 2016).

The average beach surface and volume (Figure 23 and Figure 24) reveals spatial variation from north to south, increasing towards the south. The central beaches suffer the greatest variation, with differences in area greater than 120 m^2/m and variations in volume greater than 500 m^3/m. The southern sector of São João da Caparica, Praia do Norte, Santo António da Caparica and CDS, around 20 m wide or less, are the narrowest beaches and also the less robust (≈60 m^3/m), compared to the southern beaches (≈40 m wide and ≈200 m^3/m). The maximum values reflect a nourished profile, before it reached the equilibrium profile. The survey was conducted 18 days after the nourishment was completed (survey of October 18, 2019). The minimum also returns north-south differences. Some profiles have a minimum of zero beach area and, in these cases, the beach carrying capacity is zero. The beach volume may also be zero or near zero, in these cases, the emerged beach is totally eroded and, in all tidal cycles, the water reaches the structure at least when the sea level exceeds the MSL, exposing the structure toe, which can affect its stability.

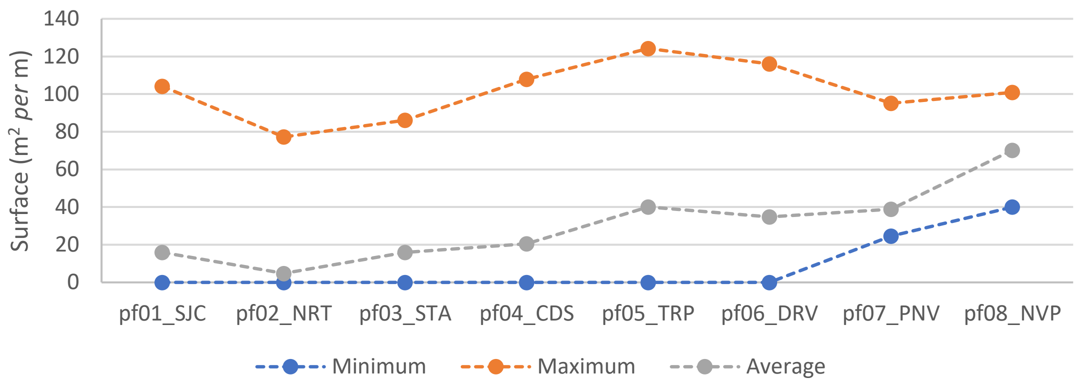

Figure 23. Statistical beach surface values (minimum, maximum and average) per profile for surveys carried out from 2011 to 2019.

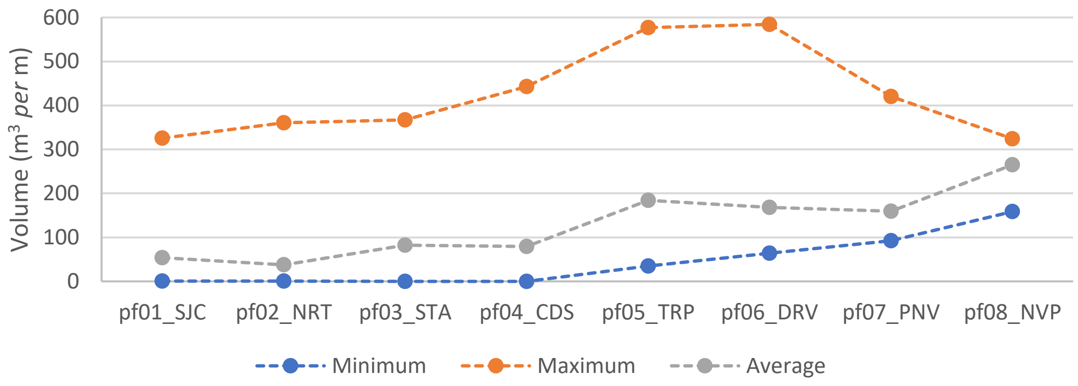

Figure 24. Statistical beach volume values (minimum, maximum and average) per profile for surveys carried out from 2011 to 2019.

Regarding to beach face slope (Figure 25), the spatial variations also reveal differences from the northern to the southern beaches. The southern sector of São João da Caparica, Praia do Norte, Santo António da Caparica and CDS, are steeper than the others, however with small differences in averages, being slopes around 0.09 and 0.08 to north and south sectors, respectively.

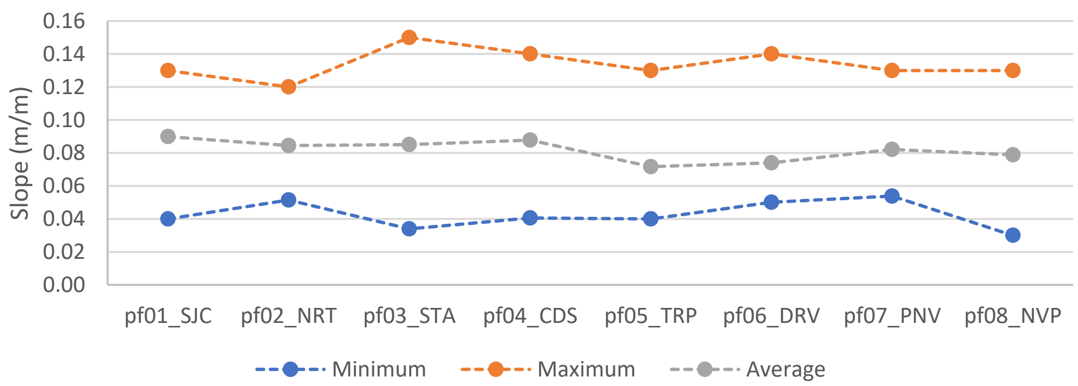

Figure 25. Statistical beach face slope values (minimum, maximum and average) per profile for surveys carried out from 2011 to 2019.

From a timeline perspective, the beach volume and surface suffer a similar variation over time (Figure 26 and Figure 27), being visible the effect of the 2014 extreme events, as well as the effect of the 2017/18 winter, with two major storms: storm Ana, on December 11, 2017; and storm Emma, on March 1, 2018.

These two storms had different intensities and effects in the study area. It is possible to assess the effects of these storms by analysing the volume timeline evolution at the southern sector of São João da Caparica (pf01_SJC) of three surveys carried out on October 2, 2017; January 19, 2018; and March 6, 2018. Between the first two surveys, in December, storm Ana hits the site with no adverse events reported. Between the last two surveys, in March, storm Emma hits the coast, this time with reports of wave overtopping, flooding and structural damage nearby the study site. The beach profile volume decreasing rate between October 2017 and January 2018 was lower (≈30%) than between January and March 2018 (≈99%), which illustrates the system different response to these two distinct storms.

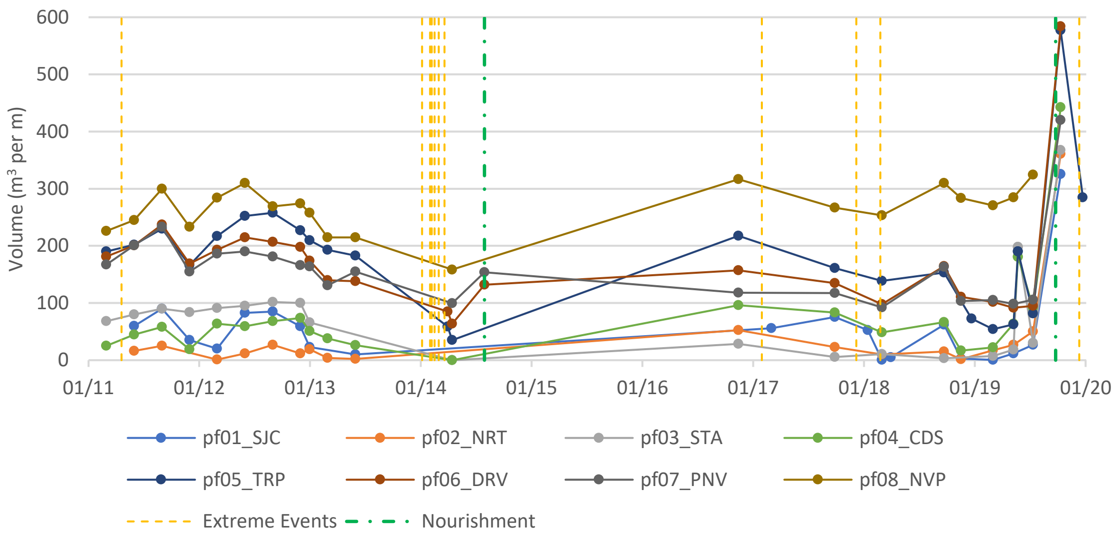

Figure 26. Time series of volume variation for the eight studied profiles, from March 2011 to December 2019.

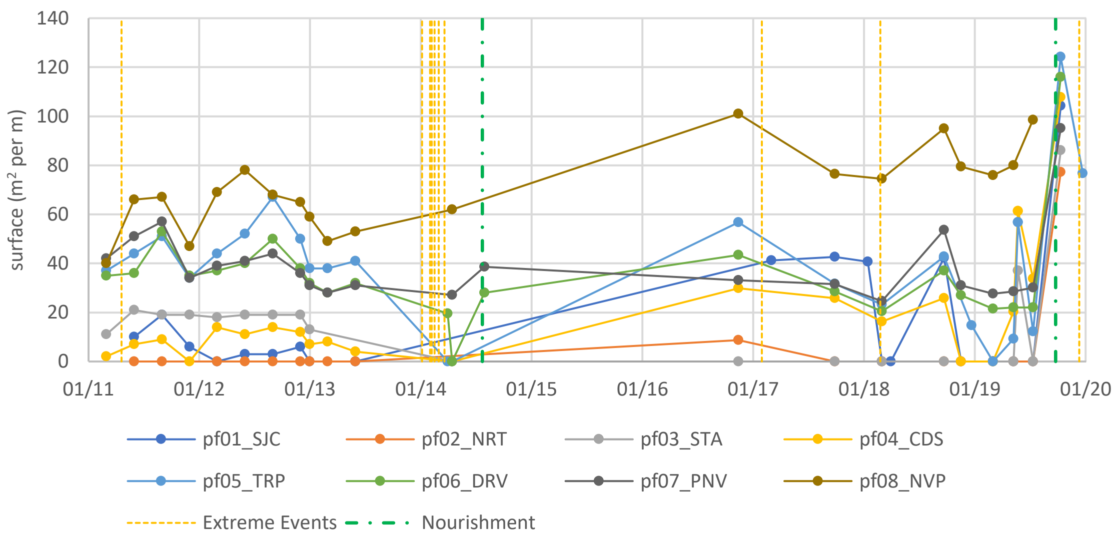

Figure 27. Time series of beach surface variation for the eight studied profiles, from March 2011 to December 2019.

During the period of analysis, two beach nourishments were performed at the study site, the last one being completed in October 2019. On October 18, 2019, a survey was conducted revealing the nourished profiles with high volumes and large surfaces. In the same year, at Traquínio-Paraíso beach (pf05_TRP), on December 30, another survey shows a high decreasing rate in volume and surface. Between surveys, three storms, Daniel, Elsa and Fabian, reached the study zone between December 15 and 22, 2019, although with no adverse events reported. It was not assessed whether the storms did not cause adverse effects because they did not have sufficient meteo-oceanographic conditions to cause damages or if that was due to the fact that the beaches were robust enough, due to nourishment. The decrease in volume and surface can also reveal the evolution to the natural profile after nourishment, however due to the storms that hit the study site it is not possible to assess what would be the profile natural evolution after nourishment.

The slope temporal variation for each profile (Figure 28) does not show a consistent response to the oceanographic forces, except in 2014. The first survey carried out after the events reveals less steep profiles. In the second survey, the profiles showed a quick change, adopting a steeper geometry.

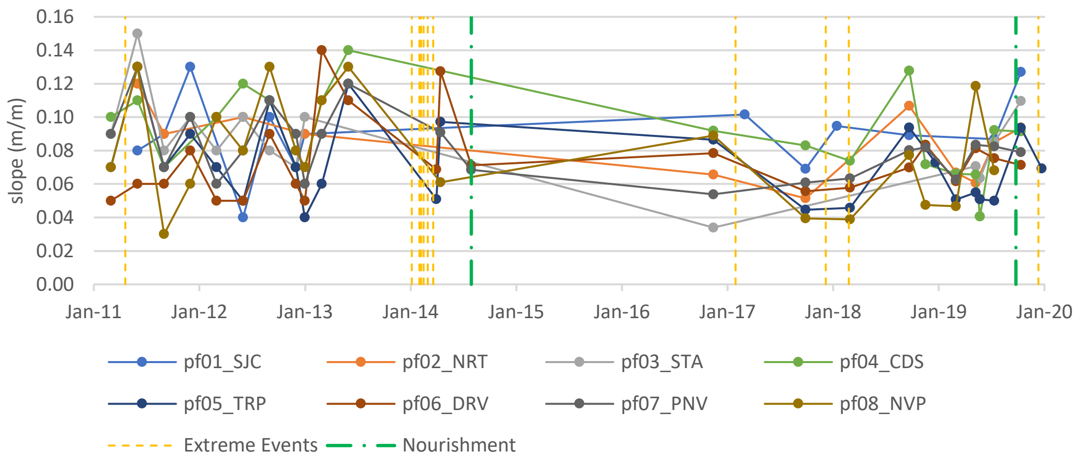

Figure 28. Timeseries of beach face slope variation for the eight studied profiles, from March 2011 to December 2019.

The profiles geometry obtained from the available surveys (

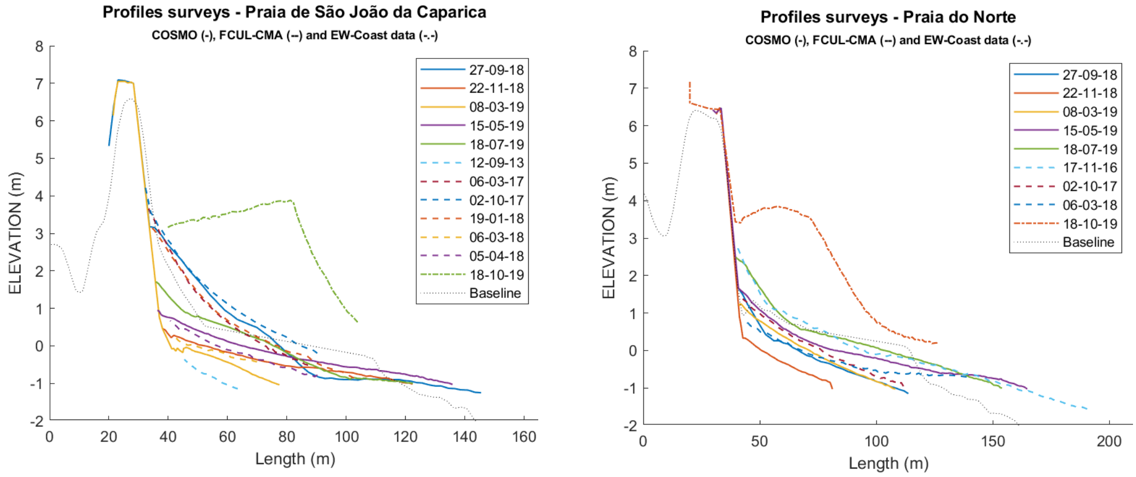

Figure 29 - Figure 32) also revealed a difference between the northern and the southern sectors. In the southern region, it is possible to see a berm formation, while the northern beaches only have a berm when the beach was nourished, in 2019. Generally, beach nourishment (in 2019) and extreme storm conditions (in 2014) produce the maximum and minimum limit boundaries in the analysed profiles. In profiles pf01_SJC, pf02_NRT, pf03_STA and pf04_CDS, the variation is more pronounced at the backshore, reaching 4 m width near the seawall. At Tarquínio-Paraíso beach, movements can be seen along the profile, where the berm crest takes on various positions and volumes.

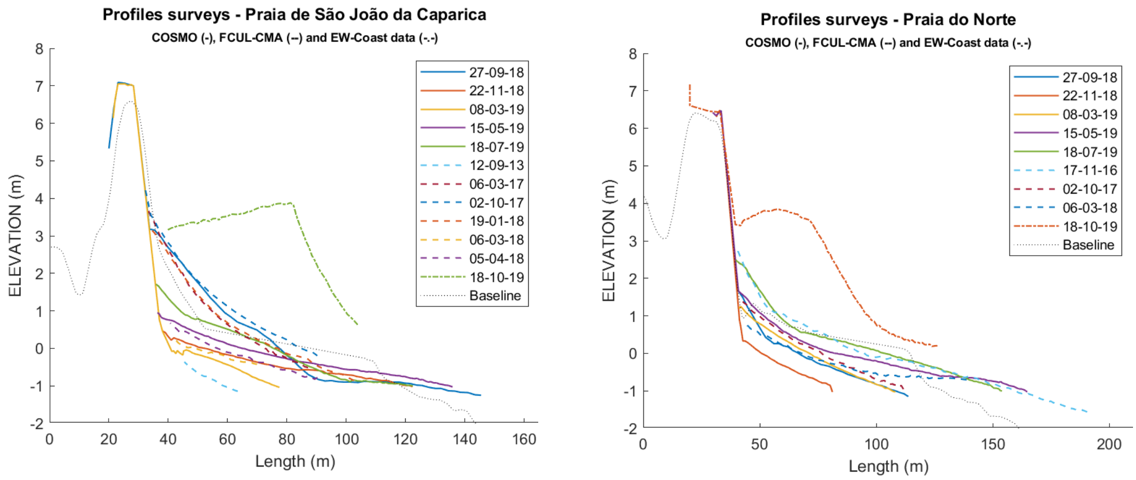

Figure 29. Beach profiles from COSMO, CMA-IDL and EW-Coast surveys. The left panel represents São João da Caparica beach (pf01_SJC) profiles and the right panel Praia do Norte beach (pf02_NRT) profiles.

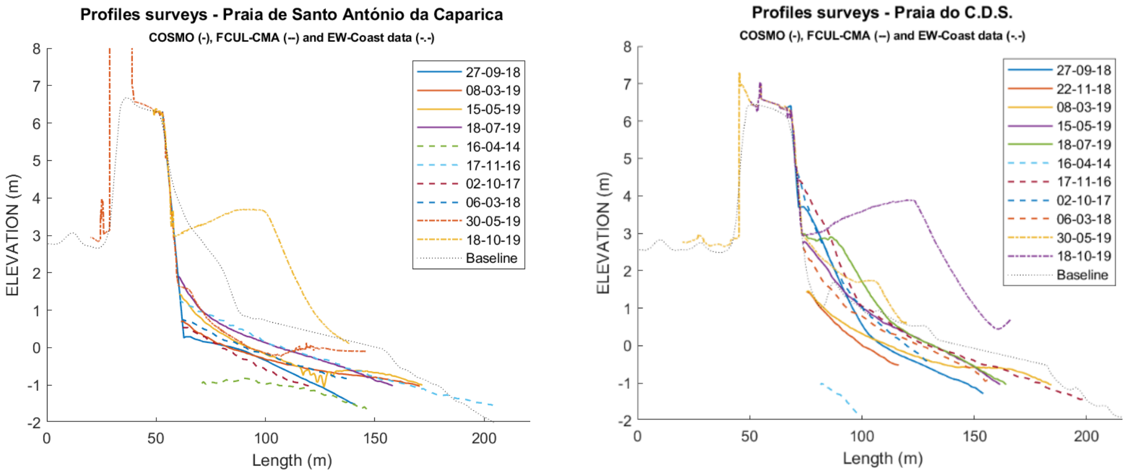

Figure 30. Beach profiles from COSMO, CMA-IDL and EW-Coast surveys. The left panel represents Santo António beach (pf03_STA) profiles and the right panel CDS beach (pf04_CDS) profiles.

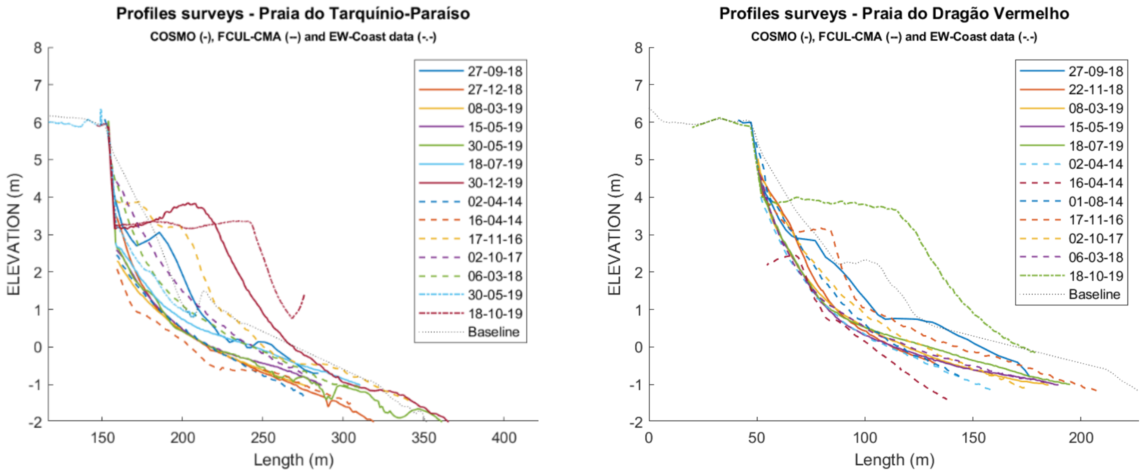

Figure 31. Beach profiles from COSMO, CMA-IDL and EW-Coast surveys. The left panel represents Traquínio-Praraíso beach (pf05_TRP) profiles and the right panel Dragão Vermelho beach (pf06_DRV) profiles.

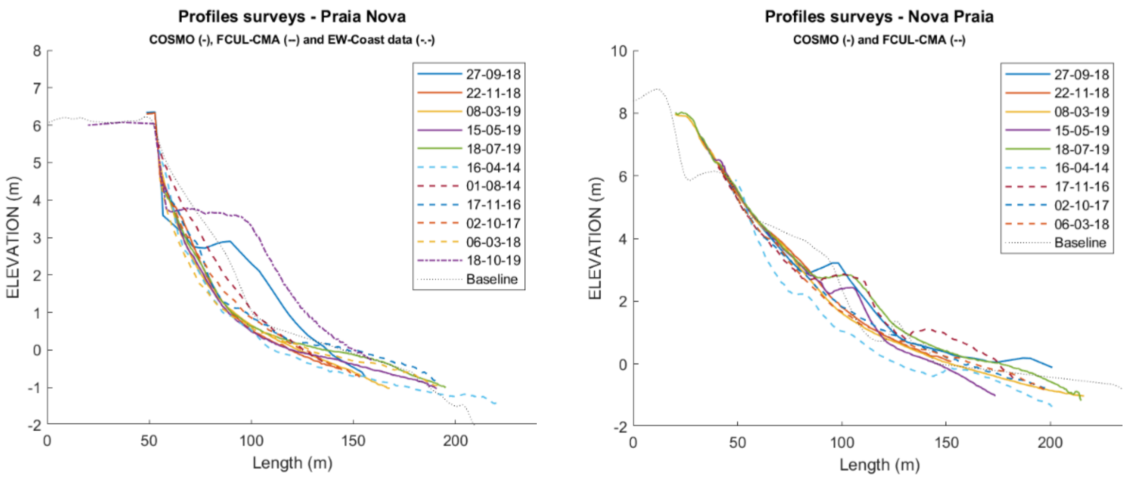

Figure 32. Beach profiles from COSMO, CMA-IDL and EW-Coast surveys. The left panel represents Praia Nova beach (pf07_PNV) profiles and the right panel Nova Praia beach (pf08_NVP) profiles.

Seasonal statistical analyses were performed with the available data for the same indicators. However, the monthly variation did not show a consistent pattern for any beach cell.

Since each beach has no space to develop landward due to the existing seawall, Masselink and Short (1993) classification cannot be applied. On these cases, when the swash zone reaches the structure, which is common during high tides and/or storms, the unnatural beach profile (beach plus seawall) can be classified as a reflective profile.

2.4. Beach states and numerical modelling implications

The numerical model experiments conducted at the local scale will use XBeach (Lashley *et al.*, 2018; Roelvink *et al.*, 2009), either non-hydrostatic or surfbeat modes, depending on the hazard impacting the area. The surfbeat mode provides a good approach to solve morphodynamic processes, including bed load and suspended sediment transport, dune face avalanching, bed update and breaching (Roelvink *et al.*, 2009), providing information to assess erosion, with relatively low computing time consumption. The non-hydrostatic mode is used to assess overtopping and overwash, since this mode solves individual waves. In this mode, the morphodynamic processes were not included.

In the south Portuguese coast, Quarteira is vulnerable to overwash, while authors expect that only highly energetic storms will erode the upper part of the beach causing damage. Therefore, two different XBeach models will be developed: one in the surfbeat mode and another in the non-hydrostatic mode, with higher focus on the second one. On the other hand, Praia de Faro is equally impacted by overwash and erosion. Therefore, the numerical efforts will aim to develop a surfbeat and non-hydrostatic mode models. For the Caparica site, the predominant risks are the wave overtopping and flooding events, since the coastline is fixed with a rock armour structure. For this case study, the modelling will be based on the numerical model XBeach non-hydrostatic one-dimensional (1D) mode.

At Caparica site, two beach states have been defined: maximum and minimum beach profiles. Maximum beach profile corresponds to a more robust beach (in volume and elevation), and the minimum beach profile corresponds to an eroded beach (in volume and elevation). These beach states were characterized by a median profile of the maximums and a median profile of the minimums, respectively. Thus, all cases scenarios will be run on the 1D non-hydrostatic mode for both beach states.

2.4.1. Quarteira

For the purposes of the project and the beach morphology characterization, the pre-storm dominant conditions are considered as similar to the survey conducted in December 17, 2019, while the post-storm conditions are similar to the December 20, 2019 survey. The average beach slope and the degree of development of the berm (wide but with a slope not completely horizontal) observed in May 2019 indicate that the beach was in a transitional state between post-storm to dominant conditions.

For modelling integration into the Bayesian network purposes, two beach states will be used: A) pre-storm conditions; and B) post-storm conditions. The surfbeat mode will use the pre-storm conditions as input topography, while the non-hydrostatic mode will use the post-storm conditions, since overwash at the area is expected only after berm depletion.

A) topography at the upper beach input of the two-dimensional (2D) surfbeat simulations will be represented by the May 2019 survey. The beach state in this survey did not completely match with the pre-storm conditions, closer to the December 17, 2019 conditions. However, this UAV survey was able to capture all topographic details that the 1D profile survey could not recognize. Moreover, preliminary model results (not presented here) indicate that for large storms, the modelled final erosion is not sensitive to the input topography, namely December 17, 2019 and May 2019. The topography information was joint with two bathymetric datasets: APA (Agência Portuguesa do Ambiente) survey from 2018 and a regional bathymetry. The first dataset, with a resolution of 10 m, covers from -0.5/-1 m to -8 m below MSL. The second one, extracted from MIRONE (Luís, 2007), has a 10 m resolution as well, and it extends up to the offshore border of the numerical grid (-25/-30 m).

B) input topography of the non-hydrostatic simulations represents the post-storm morphology. A 2D grid was created based on the nine profiles measured on December 20, 2019. In between profiles, the grid was interpolated assuming that the profiles are representative of the nearby areas. The areas outside of this survey were assumed unchangeable and only some smoothing processes were carried out in the border between the nearshore bathymetry and the profile-based area. The elevation of the urbanised area was obtained from the same UAV survey conducted in May 2019, since it did not change.

<u>Surfbeat mode.</u> A 2D grid with variable longshore and cross-shore resolutions was developed. The minimum cross-shore and alongshore resolutions were 2 m and 5 m, respectively, and the number of nodes was 67 000.

<u>Non-hydrostatic mode.</u> This numerical mode requires a notable higher resolution to provide accurate results, and therefore a new grid was built. This grid has 905 000 nodes, the cross-shore resolution ranged from 3 m to 1 m and the alongshore resolution was 5 m.

2.4.2. Faro

For the purposes of the project and beach characterization, the pre-storm dominant conditions are considered similar to the February 2018, April 2018, October 2018 and October 2019 surveys. The April 2018 survey is not considered since the upper part of the beach is not completely recovered. A highly eroded profile (post-storm of high energy events or sequence of storms) would be similar to the survey carried out in March 2018, while a beach state resulting from less severe storm (yearly average) conditions would be represented by the survey conducted in December 20, 2019.

For modelling purposes, both numerical modes will be run on the same pre-storm topographic condition. The non-hydrostatic mode will not use the post-storm condition topography since the upper beach profile slope is too steep and it would highly reduce the overwash. The topography measured in December 20, 2019 represents a good characterization of an eroded profile; however, the interpolation of the 1D profiles would not result in an accurate representation of the 2D features of the study area. Moreover, the differences between the December 2019 and the October 2018 surveys are not very significant. Therefore, the UAV survey conducted by the COSMO program in October 2018 will be implemented in the numerical model for both modes: non-hydrostatic and surfbeat. The COSMO program also surveyed nearshore areas until -13.5 m MSL. This dataset along with a regional bathymetry will be used to interpolate the 2D numerical grid (COSMO, n.d.).

Surfbeat mode. A numerical grid was built with variable longshore and cross-shore resolutions, with a minimum cross-shore and alongshore resolutions of 2 and 5 m, respectively, and 79 000 nodes.

Non-hydrostatic mode. A numerical mesh with higher resolution was built to run the simulations on this mode. The cross-shore resolution varied from 3 m to 1 m and the alongshore spacing was constant and equal to 6 m. The number of nodes was 1 415 000. For the 1D model, the resolution was refined and the cross-shore grid spacing was divided by 2.

2.4.3. Costa da Caparica

For Caparica site, the predominant risks are wave overtopping and flooding events, since the coastline is fixed with rigid structures. For this case study, the modelling will be based on the numerical model XBeach applied in the non-hydrostatic 1D mode.

Two survey profiles were chosen, which characterise maximum and minimum volumes for each beach (Table 6). The maximum profiles for all beaches were due to nourishment. The Traquínio-Paraíso profile analyses show that nourishment suffers a rapid volume decrease and, for this reason, the nourished profiles were not assumed as characteristic profiles. As was mentioned above, the beach states were characterized by a median profile of the maximums and a median profile of the minimums. In order to maintain some consistency, there was an attempt to standardize the surveys, whenever possible.

Table 6. Characteristic surveys (nourished, average and minimum beach volume) by beach profile.

Profile	Maximum		Minimum	
	Date	Source	Date	Source
pf01_SJC	27/09/2018	COSMO	22/11/2018	COSMO
pf02_NRT	18/07/2019	COSMO	08/03/2018	COSMO
pf03_STA	18/07/2019	COSMO	08/03/2018	COSMO
pf04_CDS	18/07/2019	COSMO	08/03/2018	COSMO
pf05_TRP	27/09/2018	COSMO	08/03/2018	COSMO
pf06_DRV	27/09/2018	COSMO	08/03/2018	COSMO
pf07_PNV	27/09/2018	COSMO	08/03/2018	COSMO
pf08_NVP	27/09/2018	COSMO	08/03/2018	COSMO

ACKNOWLEDGMENTS

The authors would like to acknowledge Professor Joaquim Luis for his active participation in processing and sharing bathymetric information (http://w3.ualg.pt/~jluis/mirone/main.html), as well as Municipality of Almada and Dom Luiz Institute / FCUL Geology Centre for providing survey data. They also acknowledge Instituto Hidrográfico, Puertos del Estado and APL - Administração do Porto de Lisboa, S.A., who supplied wave data. The COSMO program is also acknowledged for data obtained under *Programa de Monitorização da Faixa Costeira de Portugal Continental* (COSMO), of Agência Portuguesa do Ambiente, co-funded by the *Programa Operacional Sustentabilidade e Eficiência no Uso de Recursos (*POSEUR) and available at https://cosmo.apambiente.pt.

Project with reference ALG-LISBOA-01-145-FEDER-028657 attributed by the Portuguese Foundation for Science and Technology, IP, supported by the Regional Operational Program of Algarve and the Regional Operational Program of Lisbon in its component FEDER and the Portuguese Foundation for Science and Technology in its OE component. The authors would like to acknowledge the financial support of the Portuguese Foundation of Science and Technology (FCT) to CIMA through UIDP/00350/2020.

REFERENCES

Almeida, L.P., Vousdoukas, M. V., Ferreira, Ó., Rodrigues, B.A., Matias, A., 2012. Thresholds for storm impacts on an exposed sandy coastal area in southern Portugal. Geomorphology 143–144, 3–12. https://doi.org/10.1016/j.geomorph.2011.04.047

Blott, S.J., Pye, K., 2001. Gradistat: A grain size distribution and statistics package for the analysis of unconsolidated sediments. Earth Surf. Process. Landforms 26, 1237–1248. https://doi.org/10.1002/esp.261

Booij, N., Ris, R.C., Holthuijsen, L.H., 1999. A third-generation wave model for coastal regions: 1. Model description and validation. J. Geophys. Res. Ocean. 104, 7649–7666. https://doi.org/10.1029/98JC02622

Carapuço, M.M., Taborda, R., Silveira, T.M., Psuty, N.P., Andrade, C., Freitas, M.C., 2016. Coastal geoindicators: Towards the establishment of a common framework for sandy coastal environments. Earth-Science Rev. https://doi.org/10.1016/j.earscirev.2016.01.002

COSMO, n.d. Cosmonline - Programa de Monitorização da Faixa Costeira de Portugal Continental - COSMO [WWW Document]. Agência Portuguesa do Ambiente I.P. URL https://cosmo.apambiente.pt/ (accessed 5.21.20).

Costa, M., Silva, R., Vitorino, J., 2001. Contribuição para o Estudo do Clima de Agitação Marítima na Costa Portuguesa. 2as Jornadas Port. Eng. Costeira e Portuária - Assoc. Int. Naveg. 20.

Diogo, Z.S., Silveira, T.S., Sousa, H., Carapuço, A.M., Silva, A.N., Lira, C., Taborda, R., Andrade, C.F., 2013. Caracterização da variabilidade morfodinâmica sazonal e pós-temporal das praias da Costa da Caparica. Entregável 2.2.c, in: Criação e Implementação de Um Sistema de Monitorização No Litoral Abrangido Pela Área de Jurisdição Da Administração Da Região Hidrográfica Do Tejo.

Ferreira, J.C.R., 2016. Ordenamento Ambiental de Frentes Urbanas Litorais em Áreas Baixas de Elevado Risco e Vulnerabilidade ao Galgamento Costeiro. As Infraestruturas Verdes como Estratégia de Resiliência para as Comunidades Costeiras. FCT-UNL.

Ferreira, Ó., Plomaritis, T.A., Costas, S., 2019. Effectiveness assessment of risk reduction measures at coastal areas using a decision support system: Findings from Emma storm. Sci. Total Environ. 657, 124–135. https://doi.org/10.1016/j.scitotenv.2018.11.478

Heleno, A.J.P., 2017. Avaliação do espraiamento e inundação nas praias da Costa da Caparica: modelação com o modelo XBEACH. Instituto Superior de Engenharia de Lisboa.

Jaranović, B., 2017. Perigosidade associada a temporais no arco litoral Cascais – Cabo Espichel. Universidade de Lisboa.

Lashley, C.H., Roelvink, D., van Dongeren, A., Buckley, M.L., Lowe, R.J., 2018. Nonhydrostatic and surfbeat model predictions of extreme wave run-up in fringing reef environments. Coast. Eng. 137, 11–27. https://doi.org/10.1016/j.coastaleng.2018.03.007

Luis, J.F., 2007. Mirone: A multi-purpose tool for exploring grid data. Computers and Geosciences 33, 31–41. https://doi.org/10.1016/j.cageo.2006.05.005

Masselink, G., Short, A.D., 1993. The effect of tide range on beach morphodynamics and morphology: a conceptual beach model. J. Coast. Res. 9, nr. 3, 85–800.

Matias, A., Ferreira, Ó., Vila-Concejo, A., Morris, B., Dias, J.A., 2010. Short-term morphodynamics of non-storm overwash. Mar. Geol. 274, 69–84. https://doi.org/10.1016/j.margeo.2010.03.006

Pinto, C., Rodrigues, A., Costa, C.R., Lima, J., 2014. Registo das ocorrências no litoral - Temporal de 3 a 7 de janeiro de 2014. Relatório Técnico. APA.

Rodrigues, B.A., Matias, A., Ferreira, Ó., 2012. Overwash hazard assessment. Geol. Acta 10, 427–437. https://doi.org/10.1344/105.000001743

Roelvink, D., Reniers, A., van Dongeren, A., van Thiel de Vries, J., McCall, R., Lescinski, J., 2009. Modelling storm impacts on beaches, dunes and barrier islands. Coast. Eng. 56, 1133–1152. https://doi.org/10.1016/j.coastaleng.2009.08.006

Rogers, J.C., 1997. North Atlantic storm track variability and its association to the North Atlantic oscillation and climate variability of Northern Europe. J. Clim. 10, 1635–1647. https://doi.org/10.1175/1520-0442(1997)010<1635:NASTVA>2.0.CO;2

Santos, Â., Mendes, S., Corte-Real, J., 2014. Impacts of the storm Hercules in Portugal. Finisterra, XLiX 98, 197–220.

Santos, F.D., Lopes, A.M., Moniz, G., Ramos, L., Taborda, R., 2014. Gestão da Zona Costeira O Desafio da Mudança Relatório do Grupo de Trabalho do Litoral.

SIARL, 2017. SIARL - Sistema de Administração do Recurso Litoral [WWW Document]. Agência Port. do Ambient. I.P. URL http://siarldev.apambiente.pt/destaques.aspx (accessed 5.15.20).

Taborda, R., Andrade, C., Marques, F., Freitas, M.D.C., Rodrigues, R., Antunes, C., Pólvora, C., 2010. Plano Estratégico de Cascais Face às Alterações Climáticas: Sector Zonas Costeiras. Câmara Municipal de Cascais, Cascais.

Van Rijn, L.C., 1993. Principles of Sediment Transport. PART I, in: Rivers, Estuaries, Seas and Oceans. Aqua Publications.

Vousdoukas, M.I., Almeida, L.P.M., Ferreira, Ó., 2012a. Beach erosion and recovery during consecutive storms at a steep-sloping, meso-tidal beach. Earth Surf. Process. Landforms 37, 583–593. https://doi.org/10.1002/esp.2264

Vousdoukas, M.I., Ferreira, Ó., Almeida, L.P., Pacheco, A., 2012b. Toward reliable storm-hazard forecasts: XBeach calibration and its potential application in an operational early-warning system. Ocean Dyn. 62, 1001–1015. https://doi.org/10.1007/s10236-012-0544-6

ANNEX I

UNIVERSIDADE DO ALGARVE
CENTRO DE INVESTIGAÇÃO MARINHA E AMBIENTAL

LABORATÓRIO NACIONAL
DE ENGENHARIA CIVIL

The collected data came from several information sources, with different designations; to establish the correspondence between them, a correspondence table was created (Tab. 1).

Tab. 1 – Correspondence of designation between different sources of information.

Beach	EW-Coast	COSMO	Diogo *et al.* (2013)	CMA-IDL
São João da Caparica (south)	pf01_SJC	PCC6	PCC6	PCC6
Praia do Norte	pf02_NRT	PNT1	PCC9	PCC9
Santo António da Caparica	pf03_STA	PSC1	PCC10	PCC10
CDS	pf04_CDS	PCD1	PCC11	PCC11
Traquínio-Paraíso	pf05_TRP	PTP1	PCC12	PCC12
Dragão Vermelho	pf06_DRV	PCV1	PCC13	PCC13
Praia Nova	pf07_PNV	PNV1	PCC14	PCC14
Nova Praia	pf08_NVP	PNP1	PCC16	PCC16

Tab. 2 – Beach Slope (m/m) from collected Caparica surveys between 2011 and 2019 (several sources).

Source	Survey Date	pf01 SJC	pf02 NRT	pf03 STA	pf04 CDS	pf05 TRP	pf06 DRV	pf07 PNV	pf08 NVP
Diogo *et al*. (2013)	mar/11	No Data	No Data	0.09	0.10	0.07	0.05	0.09	0.07
Diogo *et al*. (2013)	jun/11	0.08	0.12	0.15	0.11	0.13	0.06	0.13	0.13
Diogo *et al*. (2013)	sept/11	0.09	0.09	0.08	0.07	0.07	0.06	0.07	0.03
Diogo *et al*. (2013)	dec/11	0.13	No Data	0.10	-	0.09	0.08	0.10	0.06
Diogo *et al*. (2013)	mar/12	-	-	0.08	0.10	0.07	0.05	0.06	0.10
Diogo *et al*. (2013)	jun/12	0.04	0.10	0.10	0.12	0.05	0.05	0.08	0.08
Diogo *et al*. (2013)	sept/12	0.10	-	0.08	0.11	0.11	0.09	0.11	0.13
Diogo *et al*. (2013)	dec/12	0.07	-	0.07	0.07	0.07	0.06	0.09	0.08
Diogo *et al*. (2013)	jan/13	0.09	0.09	0.10	0.07	0.04	0.05	0.06	0.07
Diogo *et al*. (2013)	mar/13	No Data	-	No Data	0.11	0.06	0.14	0.09	0.11
Diogo *et al*. (2013)	jun/13	-	-	No Data	0.14	0.12	0.11	0.12	0.13
CMA-IDL	02/04/2014	No Data	No Data	No Data	No Data	0.05	0.07	No Data	No Data
CMA-IDL	16/04/2014	No Data	No Data	-	-	0.10	0.13	0.09	0.06
CMA-IDL	01/08/2014	No Data	No Data	No Data	No Data	No Data	0.07	0.07	No Data
CMA-IDL	17/11/2016	No Data	0.07	0.03	0.09	0.09	0.08	0.05	0.09
CMA-IDL	06/03/2017	0.10	No Data	No Data	No Data	No Data	No Data	No Data	No Data
CMA-IDL	02/10/2017	0.07	0.05	-	0.08	0.04	0.06	0.06	0.04
CMA-IDL	19/01/2018	0.09	No Data	No Data	No Data	No Data	No Data	No Data	No Data
CMA-IDL	06/03/2018	-	-	-	0.07	0.05	0.06	0.06	0.04
CMA-IDL	05/04/2018	-	No Data	No Data	No Data	No Data	No Data	No Data	No Data
COSMO	27/09/2018	0.09	0.11	-	0.13	0.09	0.07	0.08	0.08
COSMO	22/11/2018	-	-	No Data	0.07	No Data	0.08	0.08	0.05
COSMO	27/12/2018	No Data	No Data	No Data	No Data	0.07	No Data	No Data	No Data
COSMO	08/03/2019	-	0.07	-	0.07	0.05	0.06	0.06	0.05
COSMO	15/05/2019	-	0.06	0.07	0.07	0.05	0.08	0.08	0.12
COSMO	30/05/2019	No Data	No Data	0.06	0.04	0.05	No Data	No Data	No Data
EW-Coast	30/05/2019	No Data	No Data	0.06	0.04	0.05	No Data	No Data	No Data
COSMO	18/07/2019	0.09	0.08	0.09	0.09	0.05	0.08	0.08	0.07
EW-Coast	18/10/2019	0.13	0.09	0.11	0.09	0.09	0.07	0.08	No Data
COSMO	30/12/2019	No Data	No Data	No Data	No Data	0.07	No Data	No Data	No Data

No Data: No available data, the survey was not carried out.

(-): Not determined by the adopted methodology.

Tab. 3 – Beach Surface (m² per m) from collected Caparica surveys between 2011 and 2019 (several sources).

Source	Survey Date	pf01 SJC	pf02 NRT	pf03 STA	pf04 CDS	pf05 TRP	pf06 DRV	pf07 PNV	pf08 NVP
Diogo *et al*. (2013)	mar/11	No Data	No Data	11.00	2.00	37.00	35.00	42.00	40.00
Diogo *et al*. (2013)	jun/11	10.00	0.00	21.00	7.00	44.00	36.00	51.00	66.00
Diogo *et al*. (2013)	sept/11	19.00	0.00	19.00	9.00	51.00	53.00	57.00	67.00
Diogo *et al*. (2013)	dec/11	6.00	No Data	19.00	0.00	34.00	35.00	34.00	47.00
Diogo *et al*. (2013)	mar/12	0.00	0.00	18.00	14.00	44.00	37.00	39.00	69.00
Diogo *et al*. (2013)	jun/12	3.00	0.00	19.00	11.00	52.00	40.00	41.00	78.00
Diogo *et al*. (2013)	sept/12	3.00	0.00	19.00	14.00	67.00	50.00	44.00	68.00
Diogo *et al*. (2013)	dec/12	6.00	0.00	19.00	12.00	50.00	38.00	36.00	65.00
Diogo *et al*. (2013)	jan/13	0.00	0.00	13.00	7.00	38.00	32.00	31.00	59.00
Diogo *et al*. (2013)	mar/13	No Data	0.00	No Data	8.00	38.00	28.00	28.00	49.00
Diogo *et al*. (2013)	jun/13	0.00	0.00	No Data	4.00	41.00	32.00	31.00	53.00
CMA-IDL	02/04/2014	No Data	No Data	No Data	No Data	0.00	19.50	No Data	No Data
CMA-IDL	16/04/2014	No Data	No Data	0.00	0.00	0.00	0.00	27.10	62.00
CMA-IDL	01/08/2014	No Data	No Data	No Data	No Data	No Data	28.00	38.60	No Data
CMA-IDL	17/11/2016	No Data	8.74	0.00	29.80	56.73	43.50	33.10	101.00
CMA-IDL	06/03/2017	41.20	No Data	No Data	No Data	No Data	No Data	No Data	No Data
CMA-IDL	02/10/2017	42.70	0.00	0.00	25.80	31.73	28.50	31.60	76.50
CMA-IDL	19/01/2018	40.70	No Data	No Data	No Data	No Data	No Data	No Data	No Data
CMA-IDL	06/03/2018	0.00	0.00	0.00	16.30	23.23	20.50	24.60	74.50
CMA-IDL	05/04/2018	0.00	No Data	No Data	No Data	No Data	No Data	No Data	No Data
COSMO	27/09/2018	42.20	0.00	0.00	25.80	42.73	37.00	53.60	95.00
COSMO	22/11/2018	0.00	0.00	No Data	0.00	No Data	27.00	31.10	79.50
COSMO	27/12/2018	No Data	No Data	No Data	No Data	14.73	No Data	No Data	No Data
COSMO	08/03/2019	0.00	0.00	0.00	0.00	0.00	21.50	27.60	76.00
COSMO	15/05/2019	0.00	0.00	0.00	20.30	9.23	22.00	28.60	80.00
COSMO	30/05/2019	No Data	No Data	37.05	61.30	56.73	No Data	No Data	No Data
EW-Coast	30/05/2019	No Data	No Data	37.05	61.30	56.73	No Data	No Data	No Data
COSMO	18/07/2019	0.00	0.00	0.00	33.80	12.23	22.00	30.10	98.50
EW-Coast	18/10/2019	104.20	77.24	86.05	107.80	124.23	116.00	95.10	No Data
COSMO	30/12/2019	No Data	No Data	No Data	No Data	76.73	No Data	No Data	No Data

No Data: No available data, the survey was not carried out.

Tab. 4 – Beach Volume (m³ per m) from collected Caparica surveys between 2011 and 2019 (several sources).

Source	Survey Date	pf01 SJC	pf02 NRT	pf03 STA	pf04 CDS	pf05 TRP	pf06 DRV	pf07 PNV	pf08 NVP
Diogo *et al*. (2013)	mar/11	No Data	No Data	68	25	190	181	167	226
Diogo *et al*. (2013)	jun/11	60	16	80	45	202	201	201	245
Diogo *et al*. (2013)	sept/11	90	25	90	58	230	237	233	300
Diogo *et al*. (2013)	dec/11	35	No Data	84	19	166	169	155	233
Diogo *et al*. (2013)	mar/12	20	1	91	64	217	193	186	284
Diogo *et al*. (2013)	jun/12	83	12	95	59	252	215	190	310
Diogo *et al*. (2013)	sept/12	85	27	102	68	258	207	181	269
Diogo *et al*. (2013)	dec/12	59	12	100	74	227	198	166	274
Diogo *et al*. (2013)	jan/13	23	19	66	51	210	174	164	258
Diogo *et al*. (2013)	mar/13	No Data	4	No Data	38	193	140	131	215
Diogo *et al*. (2013)	jun/13	10	2	No Data	26	183	138	155	215
CMA-IDL	02/04/2014	No Data	No Data	No Data	No Data	59	85	No Data	No Data
CMA-IDL	16/04/2014	No Data	No Data	0	0	35	64	99	159
CMA-IDL	01/08/2014	No Data	No Data	No Data	No Data	No Data	132	154	No Data
CMA-IDL	17/11/2016	No Data	53	29	96	218	157	118	317
CMA-IDL	06/03/2017	56	No Data	No Data	No Data	No Data	No Data	No Data	No Data
CMA-IDL	02/10/2017	76	23	5	83	161	135	118	267
CMA-IDL	19/01/2018	53	No Data	No Data	No Data	No Data	No Data	No Data	No Data
CMA-IDL	06/03/2018	0	10	11	49	139	98	92	253
CMA-IDL	05/04/2018	5	No Data	No Data	No Data	No Data	No Data	No Data	No Data
COSMO	27/09/2018	62	15	3	67	153	164	163	310
COSMO	22/11/2018	3	1	No Data	17	No Data	111	103	284
COSMO	27/12/2018	No Data	No Data	No Data	No Data	73	No Data	No Data	No Data
COSMO	08/03/2019	1	17	7	22	54	102	105	271
COSMO	15/05/2019	12	27	18	64	63	92	99	285
COSMO	30/05/2019	No Data	No Data	198	180	190	No Data	No Data	No Data
EW-Coast	30/05/2019	No Data	No Data	198	180	190	No Data	No Data	No Data
COSMO	18/07/2019	27	51	30	92	82	95	106	324
EW-Coast	18/10/2019	325	361	367	443	577	584	420	No Data
COSMO	30/12/2019	No Data	No Data	No Data	No Data	285	No Data	No Data	No Data

No Data: No available data, the survey was not carried out.